Monthly Notices
of the
ROYAL ASTRONOMICAL SOCIETY

Mon. Not. R. Astron. Soc. **410,** 585–611 (2011) doi:10.1111/j.1365-2966.2010.17474.x

Fourteen months of observations of the possible super-Chandrasekhar mass Type Ia Supernova 2009dc

Jeffrey M. Silverman,★† Mohan Ganeshalingam, Weidong Li, Alexei V. Filippenko, Adam A. Miller and Dovi Poznanski

Department of Astronomy, University of California, Berkeley, CA 94720-3411, USA

Accepted 2010 July 31. Received 2010 July 30; in original form 2010 March 11

ABSTRACT

In this paper, we present and analyse optical photometry and spectra of the extremely luminous and slowly evolving Type Ia supernova (SN Ia) 2009dc, and offer evidence that it is a super-Chandrasekhar mass (SC) SN Ia and thus has a SC white dwarf (WD) progenitor. Optical spectra of SN 2007if, a similar object, are also shown. SN 2009dc had one of the most slowly evolving light curves ever observed for a SN Ia, with a rise time of $\sim$23 d and $\Delta m_{15}(B) = 0.72$ mag. We calculate a lower limit to the peak bolometric luminosity of $\sim 2.4 \times 10^{43}$ erg s^{-1}, though the actual value is likely almost 40 per cent larger. Optical spectra of SN 2009dc and SN 2007if obtained near maximum brightness exhibit strong C II features (indicative of a significant amount of unburned material), and the post-maximum spectra are dominated by iron-group elements (IGEs). All of our spectra of SN 2009dc and SN 2007if also show low expansion velocities. However, we see no strong evidence in SN 2009dc for a velocity 'plateau' near maximum light like the one seen in SN 2007if. The high luminosity and low expansion velocities of SN 2009dc lead us to derive a possible WD progenitor mass of more than 2 M$_\odot$ and a ^{56}Ni mass of about 1.4–1.7 M$_\odot$. We propose that the host galaxy of SN 2009dc underwent a gravitational interaction with a neighbouring galaxy in the relatively recent past. This may have led to a sudden burst of star formation which could have produced the SC WD progenitor of SN 2009dc and likely turned the neighbouring galaxy into a 'post-starburst galaxy'. No published model seems to match the extreme values observed in SN 2009dc, but simulations do show that such massive progenitors can exist (likely as a result of the merger of two WDs) and can possibly explode as SC SNe Ia.

Key words: supernovae: general – supernovae: individual: SN 2009dc – supernovae: individual: SN 2007if – supernovae: individual: SN 2003fg – supernovae: individual: SN 2006gz.

1 INTRODUCTION

Type Ia supernovae (SNe Ia) are differentiated from other types of SNe by the absence of hydrogen and the presence of broad absorption from Si II λ6355 in their optical spectra (for a review see Filippenko 1997). SNe Ia have been used to measure cosmological parameters to high precision (e.g. Kowalski et al. 2008; Hicken et al. 2009; Kessler et al. 2009; Amanullah et al. 2010), as well as to discover the accelerating expansion of the Universe (Riess et al. 1998; Perlmutter et al. 1999). Broadly speaking, SNe Ia are the result of thermonuclear explosions of C–O white dwarfs (WDs) resulting from either the accretion of matter from a non-degenerate companion star (e.g. Whelan & Iben 1973) or the merger of two degenerate objects (e.g. Iben & Tutukov 1984; Webbink 1984). However, the nature of the companion and the details of the explosion itself are both still quite uncertain.

The cosmological utility of SNe Ia comes from the fact that they are standardizable candles (i.e. their luminosities at peak can be calibrated). This naively seems reasonable since SNe Ia should all have the same amount of fuel and the same trigger point: they should all explode when a WD nearly reaches the Chandrasekhar mass of $\sim$1.4 M$_\odot$.

In 2003, SNLS-03D3bb (also known as SN 2003fg) was discovered (Howell et al. 2006) and was shown to be a SN Ia that was overluminous by about a factor of 2, and had a slowly declining light curve, quite low expansion velocities and unburned material present

★E-mail: jsilverman@astro.berkeley.edu
†Marc J. Staley Fellow.

in near-maximum light spectra. This last observation implies that a layer of carbon and oxygen from the progenitor existed on top of the burned silicon layer. In SNe Ia, carbon is usually extremely weak or completely absent (even at very early times) in optical and infrared (IR) spectra, although it has been (sometimes tentatively) identified in a few other cases (e.g. Branch et al. 2003; Marion et al. 2006; Thomas et al. 2007; Foley et al. 2010). Howell et al. (2006) suggest that all of the oddities seen in SN 2003fg could be explained if its progenitor WD had a mass greater than the canonical upper limit for WDs of $\sim$1.4 $M_{\odot}$, a so-called 'super-Chandrasekhar mass' (SC) WD.

Hicken et al. (2007) then presented data on SN 2006gz which shared some of the strange properties of SN 2003fg, and they concluded that SN 2006gz must have come from a WD merger leading to an SC SN Ia. Recently, Scalzo et al. (2010) published observations of SN 2007if which is yet another example of this emerging class of possible SC SNe Ia. They not only observed low expansion velocities, but also saw a plateau in the expansion velocity near maximum brightness which they interpret as evidence for the SN ejecta running into a shell of material. The accurately determined total mass of the SN 2007if system is well above the Chandrasekhar mass.

Recently, it was pointed out that there might be another member of this SC SN Ia class, SN 2009dc (Harutyunyan, Elias-Rosa & Benetti 2009; Marion et al. 2009; Yamanaka et al. 2009). SN 2009dc was discovered 15.8 arcsec west and 20.8 arcsec north of the nucleus of the S0 galaxy UGC 10064 by Puckett et al. (2009) on 2009 Apr. 9.31 (UT dates are used throughout this paper), although in Section 3.1 we will show a detection of the SN $\sim$5 days earlier. It is located at $\alpha_{J2000} = 15^{h}51^{m}12\overset{s}{.}12$ and $\delta_{J2000} = +25^{\circ}42'28\overset{''}{.}0$; the SN and its host are shown in Fig. 1. No object was visible in our data at the position of the SN on 2009 Mar. 28 to a limiting magnitude of $\sim$19.5, so the actual explosion date was almost certainly between Mar. 28 and Apr. 4.

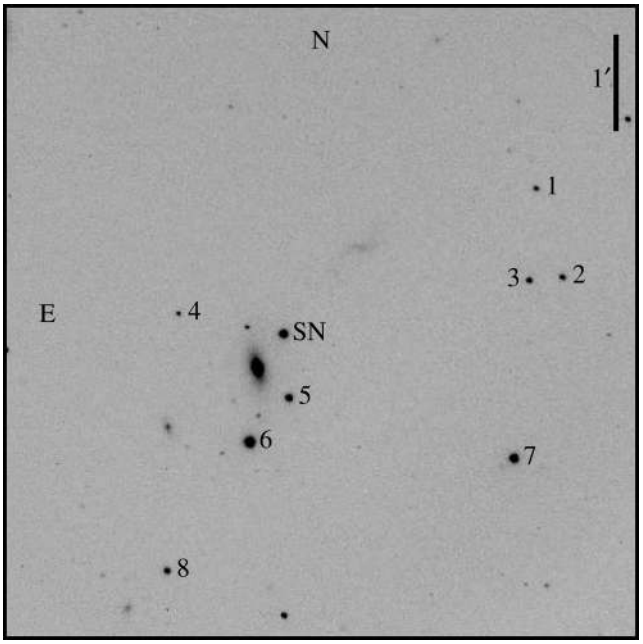

Figure 1. KAIT image of SN 2009dc and its host galaxy, UGC 10064. The field of view is 6.7 × 6.7 arcmin^2. SN 2009dc is labelled along with the comparison stars used for differential photometry. The scale of the image is marked in the top right; north is up and east is to left. The SN is sufficiently far from its host galaxy that template subtraction was not performed when conducting photometry.

Harutyunyan et al. (2009) obtained a spectrum of SN 2009dc one week after the announced discovery date and showed it to be an SN Ia before maximum light. They also noted that SN 2009dc spectroscopically resembled the SC SN Ia candidate SN 2006gz (Hicken et al. 2007) at this time, but with a much lower expansion velocity as derived from the Si II λ6355 absorption feature. Three days later, nearly simultaneous optical and IR spectra were obtained by Marion et al. (2009), covering a wavelength range of 0.36 to 1.3 μm. They again note some similarities to (as well as differences from) SN 2006gz, as well as similarities with the possible SC SN Ia 2003fg (Howell et al. 2006).

Yamanaka et al. (2009) presented early-time optical and near-IR observations of SN 2009dc and showed that it did indeed share many of the properties seen in both SN 2003fg and SN 2006gz, suggesting that it too is a possible SC SN Ia. Furthermore, Tanaka et al. (2010) published spectropolarimetry of SN 2009dc which indicated that the explosion was quite spherically symmetric.

In this paper we present and analyse our own optical photometric and spectroscopic data for SN 2009dc (as well as spectra of SN 2007if) with the goal of more definitively answering the question of whether SN 2009dc and SN 2007if were truly SC SNe Ia. We show some of the most precise data on the rise time of a possible SC SN Ia ever published, as well as some of the latest-time photometric and spectral observations of a member of this class. In Section 2 we describe our observations and data reduction, and in Section 3 we discuss our analysis of the photometry and spectra of SN 2009dc (and its host galaxy) and SN 2007if. We attempt to robustly calculate physical parameters of SN 2009dc using a variety of methods and compare them to theoretical predictions in Section 4. Finally, in Section 5, we summarize our conclusions and ruminate about the future.

2 OBSERVATIONS AND DATA REDUCTION

2.1 Photometry

Observations of SN 2009dc began on 2009 Apr. 17, about one week before maximum *B*-band brightness, in *BVRI* filters using the 0.76-m Katzman Automatic Imaging Telescope (KAIT; Filippenko et al. 2001) and the 1-m Nickel telescope, both at Lick Observatory. We continued to follow SN 2009dc for over 5 months until 2009 Sept. 26, when it reached the western limit of both telescopes in the early evening. We obtained late-time *gVRI* images of SN 2009dc using the dual-arm Low-Resolution Imaging Spectrometer (LRIS; Oke et al. 1995) with the 10-m Keck I telescope on 2010 Feb. 6 (281 d past maximum), *BRI* images using the DEIMOS spectrograph (Faber et al. 2003) mounted on the 10-m Keck II telescope on 2010 Jun. 12 (403 d past maximum) and *V*-band images again using LRIS on 2010 Jun. 13.

Our optical photometry is complemented with data taken from the UltraViolet Optical Telescope (UVOT) on the *Swift* Observatory in the *U*, *B*, *V*, *UVW*1, *UVM*2 and *UVW*2 filters. We downloaded seven epochs of observations from the *Swift* archives.

Our early-time optical images were reduced using a pipeline developed for KAIT and Nickel data (Ganeshalingam et al. 2010). The images were bias subtracted and flatfielded at the telescope. Given the distance of SN 2009dc from the host galaxy, we did not find it necessary to attempt galaxy subtraction. We performed differential photometry using point spread function (PSF) fitting photometry on SN 2009dc and several comparison stars in the field with

Table 1. Comparison stars for the SN 2009dc field.

Star	α_{J2000}	δ_{J2000}	B (mag)	V (mag)	R (mag)	I (mag)	N_{calib}
SN	15:51:12.12	+25:42:28.0					
1	15:51:00.40	+25:44:00.1	18.769 (010)	17.418 (006)	16.503 (005)	15.744 (011)	9
2	15:50:59.16	+25:43:04.7	17.501 (008)	16.957 (006)	16.608 (004)	16.236 (008)	12
3	15:51:00.72	+25:43:02.5	18.126 (009)	16.816 (004)	15.940 (004)	15.228 (008)	10
4	15:51:16.96	+25:42:40.6	18.671 (006)	17.805 (005)	17.249 (006)	16.734 (011)	11
5	15:51:11.83	+25:41:48.3	16.661 (007)	15.872 (004)	15.406 (003)	14.984 (009)	13
6	15:51:13.64	+25:41:20.5	15.383 (007)	14.471 (004)	13.935 (003)	13.460 (009)	13
7	15:51:01.38	+25:41:11.2	15.892 (007)	15.200 (005)	14.808 (003)	14.420 (010)	13
8	15:51:17.44	+25:39:59.6	17.156 (006)	16.534 (004)	16.174 (004)	15.790 (008)	13

Note. 1σ uncertainties are in parentheses, in units of 0.001 mag.

Table 2. Early-time *BVRI* photometry of SN 2009dc.

JD	B (mag)	V (mag)	R (mag)	I (mag)	Telescope
245 4925.95	...	...	18.824 (177)	...	KAIT
245 4938.98	15.670 (030)	15.638 (020)	15.596 (020)	15.718 (030)	KAIT
245 4939.95	15.549 (030)	15.541 (020)	15.500 (020)	15.577 (030)	Nickel
245 4940.92	15.474 (030)	15.472 (030)	15.430 (030)	15.524 (030)	Nickel
245 4940.93	15.511 (030)	15.495 (020)	15.475 (020)	15.608 (030)	KAIT
245 4942.95	15.455 (030)	15.409 (020)	15.376 (020)	15.529 (030)	KAIT
245 4946.97	15.383 (030)	15.327 (020)	15.272 (020)	15.450 (030)	KAIT
245 4948.87	15.369 (030)	15.350 (020)	15.288 (020)	15.454 (030)	KAIT
245 4951.92	15.449 (030)	15.386 (020)	15.311 (020)	15.449 (030)	KAIT
245 4957.97	15.770 (030)	15.535 (020)	15.423 (020)	15.537 (030)	KAIT
245 4959.85	15.930 (030)	15.610 (020)	15.464 (020)	15.554 (030)	KAIT
245 4960.92	16.004 (030)	15.591 (020)	15.476 (020)	15.593 (030)	KAIT
245 4962.93	16.137 (036)	15.656 (024)	15.543 (026)	15.633 (084)	KAIT
245 4964.90	16.322 (030)	15.762 (020)	15.584 (020)	15.568 (030)	KAIT
245 4966.93	16.528 (030)	15.846 (020)	15.642 (020)	15.562 (030)	KAIT
245 4966.95	16.478 (030)	15.839 (020)	15.611 (020)	15.481 (030)	Nickel
245 4968.89	16.677 (030)	15.926 (020)	15.675 (020)	15.565 (030)	KAIT
245 4970.88	...	16.029 (086)	15.696 (053)	...	KAIT
245 4971.92	16.880 (030)	16.054 (020)	15.701 (024)	15.500 (030)	Nickel
245 4972.89	16.972 (030)	16.106 (020)	15.748 (020)	15.579 (030)	KAIT
245 4974.88	17.154 (030)	16.202 (020)	15.799 (020)	15.557 (030)	KAIT
245 4975.87	17.188 (030)	16.239 (020)	15.797 (020)	15.526 (030)	Nickel
245 4977.90	17.384 (030)	16.334 (020)	15.874 (020)	15.659 (030)	KAIT
245 4981.89	17.650 (047)	16.488 (020)	16.009 (020)	15.707 (030)	KAIT
245 4989.83	18.045 (078)	16.893 (027)	16.364 (020)	15.979 (034)	KAIT
245 4989.87	17.891 (062)	16.855 (030)	16.333 (030)	15.951 (030)	Nickel
245 4993.85	18.128 (080)	16.943 (041)	16.480 (021)	16.167 (030)	KAIT
245 4993.90	18.032 (042)	16.960 (022)	16.483 (020)	16.093 (030)	Nickel
245 4999.81	18.188 (057)	17.083 (026)	16.696 (020)	...	KAIT
245 4999.83	18.153 (037)	17.102 (020)	16.675 (027)	16.315 (030)	Nickel
245 5004.78	18.208 (033)	17.180 (033)	16.835 (028)	16.478 (034)	Nickel
245 5007.84	18.265 (030)	17.289 (022)	16.913 (027)	16.540 (031)	Nickel
245 5009.80	18.254 (089)	17.277 (029)	16.944 (022)	16.677 (039)	KAIT
245 5014.83	18.449 (084)	17.344 (057)	17.151 (021)	16.761 (038)	KAIT
245 5015.83	18.370 (046)	17.427 (022)	17.132 (031)	16.794 (042)	Nickel

the DAOPHOT package in IRAF.[1] The output instrumental magnitudes were calibrated to the standard Johnson *BV* and Cousins *RI* system using colour terms derived from many photometric nights. The comparison stars were calibrated against Landolt (1992) standard stars using 13 photometric epochs to achieve a root mean square (rms) of <0.01 mag. The comparison stars are identified in Fig. 1 with corresponding photometry in Table 1. To estimate the uncertainty in our photometry pipeline, we add artificial stars with the same magnitude and PSF as the SN to each data image at positions of similar background brightness; the rms of doing this procedure 20 times is taken as the uncertainty. The photometric uncertainty is added in quadrature to the calibration error to produce our final uncertainty, adopting an error floor of 0.03 mag for *B* and *I* and 0.02 mag for *V* and *R* to account for slight systematic differences between the KAIT and Nickel photometry. Our final photometry of SN 2009dc is presented in Table 2.

[1] IRAF: the Image Reduction and Analysis Facility is distributed by the National Optical Astronomy Observatory, which is operated by the Association of Universities for Research in Astronomy (AURA) under cooperative agreement with the National Science Foundation (NSF).

Table 2 – *continued*

JD	*B* (mag)	*V* (mag)	*R* (mag)	*I* (mag)	Telescope
245 5019.85	18.377 (106)	17.432 (043)	17.247 (040)	16.937 (036)	Nickel
245 5022.74	18.271 (097)	17.581 (047)	17.295 (025)	16.890 (050)	KAIT
245 5025.83	18.585 (049)	17.607 (069)	17.431 (059)	17.176 (053)	Nickel
245 5027.69	18.502 (054)	17.625 (041)	17.439 (035)	17.243 (036)	KAIT
245 5032.69	18.512 (089)	17.770 (043)	17.570 (020)	17.343 (036)	KAIT
245 5032.85	18.607 (032)	17.726 (020)	17.588 (025)	17.317 (043)	Nickel
245 5034.73	18.678 (030)	17.779 (036)	17.643 (028)	17.425 (046)	Nickel
245 5037.69	18.686 (053)	17.805 (045)	17.725 (023)	17.455 (035)	KAIT
245 5040.77	18.756 (030)	17.902 (023)	17.800 (021)	17.504 (030)	Nickel
245 5042.68	18.646 (062)	18.060 (077)	17.908 (066)	17.690 (111)	KAIT
245 5042.77	18.844 (060)	17.912 (037)	17.886 (035)	17.586 (037)	Nickel
245 5044.73	18.788 (041)	17.971 (043)	17.946 (028)	17.666 (053)	Nickel
245 5047.68	19.035 (151)	17.965 (055)	18.007 (116)	17.646 (057)	KAIT
245 5047.73	18.900 (142)	18.075 (076)	18.026 (049)	17.825 (119)	Nickel
245 5052.68	18.992 (115)	18.208 (050)	18.178 (040)	17.860 (140)	KAIT
245 5054.77	...	18.231 (083)	18.256 (132)	17.909 (133)	Nickel
245 5057.69	18.967 (174)	18.233 (136)	18.198 (170)	18.064 (176)	KAIT
245 5059.71	19.026 (048)	18.241 (036)	18.309 (041)	18.065 (044)	Nickel
245 5062.67	19.087 (120)	18.323 (049)	18.364 (135)	18.227 (174)	KAIT
245 5064.70	19.070 (051)	18.339 (045)	18.484 (038)	18.093 (050)	Nickel
245 5067.66	19.061 (086)	18.324 (067)	18.462 (068)	18.307 (172)	KAIT
245 5068.69	19.144 (045)	18.368 (024)	18.559 (065)	18.285 (080)	Nickel
245 5071.69	19.166 (052)	18.427 (033)	18.632 (039)	18.283 (090)	Nickel
245 5072.66	19.164 (142)	18.512 (075)	18.653 (085)	18.437 (130)	KAIT
245 5074.69	19.249 (098)	18.497 (044)	18.717 (061)	18.313 (082)	Nickel
245 5077.65	...	18.725 (082)	...	...	KAIT
245 5082.65	19.163 (089)	18.789 (088)	19.011 (188)	18.618 (143)	KAIT
245 5087.64	...	18.919 (171)	...	...	KAIT
245 5090.68	19.444 (052)	18.765 (037)	19.219 (091)	18.800 (081)	Nickel
245 5093.66	19.528 (078)	18.820 (043)	19.176 (086)	18.867 (144)	Nickel
245 5100.66	19.665 (061)	18.954 (095)	19.441 (151)	...	Nickel

Note. 1σ uncertainties are in parentheses, in units of 0.001 mag.

Table 3. Late-time photometry of SN 2009dc.

JD	Phase[a]	Telescope	Filter	Exposure (s)	Mag	σ
245 5202.07	250	Nickel	*B*	600	21.868	0.268
	250	Nickel	*V*	360	21.016	0.320
245 5233.10	281	Keck/LRIS	*g*	180	21.894	0.050
	281	Keck/LRIS	*V*	180	21.988	0.042
	281	Keck/LRIS	*R*	60	22.600	0.084
	281	Keck/LRIS	*I*	120	21.483	0.060
245 5359.05	403	Keck/DEIMOS	*B*	360	25.010	0.120
	403	Keck/DEIMOS	*R*	450	24.987	0.143
	403	Keck/DEIMOS	*I*	450	23.746	0.185
245 5360.10	404	Keck/LRIS	*V*	540	24.834	0.152

[a]Rest-frame days relative to the date of *B*-band maximum brightness.

Late-time data obtained at the Keck I and II telescopes were bias subtracted and flatfielded using standard imaging techniques. Differential photometry was performed using PSF fitting photometry on the SN and comparison stars that were not saturated, but also detected in our calibration images obtained with the Nickel telescope. Calibrations for the *g* band were obtained using the transformations presented by Jester et al. (2005). In cases where all of the field stars from our Nickel calibration were saturated, calibrations for fainter stars in the field were obtained from the Sloan Digital Sky Survey (SDSS) and transformed into *BVRI* using transformations for stars from Jester et al. (2005). Colour-term corrections were not applied. We include a systematic error of 0.03 mag in all bands. Our final late-time photometry of SN 2009dc is presented in Table 3, which also includes an epoch of photometry obtained with the Nickel.

We downloaded the Level-2 UVOT data from the *Swift* archive. Images taken during the same pointing were registered and stacked to produce deeper images. We performed aperture photometry using the recipes prescribed by Li et al. (2006) for the optical data and Poole et al. (2008) for the UV data. We modified the *U*-band data to be in the Johnson–Cousins system using the colour corrections found in Li et al. (2006). In general, the UVOT *B* and *V* photometry is in good agreement with the photometry from our ground-based

Table 4. UVOT photometry of SN 2009dc.

JD	Filter	Mag	σ	JD	Filter	Mag	σ
245 4946.57	UVW2	17.338	0.044	245 4946.57	*U*	14.720	0.017
245 4951.85	UVW2	17.756	0.079	245 4952.21	*U*	15.124	0.010
245 4952.22	UVW2	17.987	0.073	245 4955.72	*U*	15.506	0.022
245 4955.72	UVW2	18.246	0.053	245 4960.61	*U*	16.016	0.027
245 4960.61	UVW2	18.741	0.066	245 4980.35	*U*	17.890	0.066
245 4980.35	UVW2	20.220	0.146	245 4984.44	*U*	18.070	0.088
245 4984.44	UVW2	20.314	0.177	245 4946.57	*B*	15.324	0.017
245 4946.58	UVM2	17.261	0.027	245 4955.72	*B*	15.630	0.017
245 4955.73	UVM2	18.346	0.058	245 4960.61	*B*	15.935	0.019
245 4960.61	UVM2	18.884	0.075	245 4980.35	*B*	17.542	0.042
245 4980.35	UVM2	19.986	0.135	245 4984.44	*B*	17.739	0.055
245 4984.45	UVM2	19.586	0.138	245 4946.58	*V*	15.286	0.028
245 4946.53	UVW1	16.041	0.032	245 4955.73	*V*	15.489	0.027
245 4951.71	UVW1	16.537	0.035	245 4960.61	*V*	15.587	0.028
245 4955.65	UVW1	16.965	0.035	245 4980.35	*V*	16.550	0.044
245 4960.27	UVW1	17.404	0.042	245 4984.45	*V*	16.714	0.058
245 4980.20	UVW1	18.644	0.077				
245 4984.17	UVW1	18.812	0.099				

telescopes to within ± 0.05 mag. The UVOT *B*-band data are systemically brighter, which could possibly be attributed to galaxy light falling within our aperture. Our results are given in Table 4.

We did not follow the photometric behaviour of SN 2007if, another SC SN Ia candidate, but we do present spectroscopic observations (see Section 2.2). Throughout the rest of the paper we adopt 2007 Sept. 5.4 as the date of *B*-band maximum brightness and 0.07416 as the redshift (z) of SN 2007if, both taken from Scalzo et al. (2010).

2.2 Spectroscopy

Beginning about a week before maximum brightness, optical spectra of SN 2009dc were obtained mainly using the dual-arm Kast spectrograph (Miller & Stone 1993) on the Lick 3-m Shane telescope. Two spectra were also obtained using LRIS on Keck I. Our last spectral observation occurred 281 d after *B*-band maximum.

The Kast spectra all used a 2 arcsec wide slit, a 600/4310 grism on the blue side and a 300/7500 grating on the red side, yielding full-width at half-maximum (FWHM) resolutions of $\sim$4 and $\sim$10 Å, respectively. The LRIS spectrum was obtained with a 1 arcsec slit, a 600/4000 grism on the blue side, and a 400/8500 grating on the red side, resulting in FWHM resolutions of $\sim$4 and $\sim$6 Å, respectively. All observations were aligned along the parallactic angle to reduce differential light losses (Filippenko 1982). Table 5 summarizes the spectral data of SN 2009dc presented in this paper.

We obtained three spectra of SN 2007if using LRIS. For the first two LRIS spectra, we used a 400/3400 grism on the blue side and a 400/8500 grating on the red side, resulting in FWHM resolutions of $\sim$6 Å on both sides, while the final spectrum of SN 2007if was obtained with a 600/4000 grism on the blue side, giving a resolution of $\sim$4 Å. In all cases, the long, 1 arcsec-wide slit was aligned along the parallactic angle to reduce differential light losses. Table 6 summarizes the spectral data on SN 2007if presented here. We also note that our last spectrum of SN 2007if (from 2007 Dec. 13) was taken under non-ideal observing conditions (clouds were present and the atmospheric seeing was poor), and thus its spectrophotometric accuracy is not as good as that of the other observations.

Table 5. Journal of spectroscopic observations of SN 2009dc.

UT date	Age[a]	Range (Å)	Airmass[b]	Exp (s)
2009 Apr. 18.5	−7	3500–9900	1.06	1500
2009 May 31.3	35	3500–102 00	1.03	1500
2009 Jun. 17.5[c]	52	3400–10200	1.56	250/200[d]
2009 Jun. 29.3	64	3500–10200	1.08	2100
2009 Jul. 16.3	80	3500–10200	1.29	2100
2009 Jul. 23.2	87	3500–10200	1.10	2100
2009 Jul. 28.3	92	3500–10200	1.33	2100
2009 Aug. 14.2	109	3500–10000	1.31	2400
2010 Feb. 6.6[c]	281	3500–10200	1.19	3×(630/600)[d]

[a]Rest-frame days relative to the date of *B*-band brightness maximum, 2009 Apr. 25.4 (see Section 3.1).
[b]Airmass at midpoint of exposure.
[c]These observations used LRIS (Oke et al. 1995) on the 10-m Keck I Telescope. The others used the Kast spectrograph on the Lick 3-m Shane Telescope (Miller & Stone 1993).
[d]The blue side was exposed longer than the red side due to the relatively long readout time of the red-side CCD in LRIS.

Table 6. Journal of spectroscopic observations of SN 2007if.

UT date	Age[a]	Range (Å)	Airmass[b]	Exp. (s)
2007 Oct. 15.4	37	3300–9200	1.03	1200
2007 Nov. 12.2	63	3300–9150	1.49	1200
2007 Dec. 13.2[c]	92	3300–9150	1.01	1200

[a]Rest-frame days relative to the date of *B*-band maximum brightness, 2007 Sept. 5.4 (Scalzo et al. 2010).
[b]Airmass at midpoint of exposure.
[c]This observation used a slightly higher resolution grism for the blue side.

All spectra were reduced using standard techniques (e.g. Foley et al. 2003). Routine CCD processing and spectrum extraction were completed with IRAF, and the data were extracted with the optimal algorithm of Horne (1986). We obtained the wavelength scale from low-order polynomial fits to calibration-lamp spectra. Small wavelength shifts were then applied to the data after cross-correlating a template sky to the night-sky lines that were extracted with the SN. Using our own IDL routines, we fit spectrophotometric standard-star

spectra to the data in order to flux calibrate our spectra and to remove telluric lines (Wade & Horne 1988; Matheson et al. 2000). Information regarding both our photometric and spectroscopic data (such as observing conditions, instrument, reducer, etc.) was obtained from our SN data base (SNDB). The SNDB uses the popular open-source software stack known as LAMP: the Linux operating system, the Apache webserver, the MySQL relational data base management system and the PHP server-side scripting language (see Silverman et al., for further details).

3 ANALYSIS

3.1 Light curves

We present our final optical *BVRI* light curves of SN 2009dc in Fig. 2. We include for comparison a 'normal' Type Ia SN 2005cf (Wang et al. 2009b), another SC SN Ia candidate SN 2006gz (Hicken et al. 2007), the 'standard overluminous' Type Ia SN 1991T (Lira et al. 1998) and the peculiar SN 2002cx-like SN 2005hk (Phillips et al. 2007).

The light curves of SN 2009dc have many features which are noticeably distinct from most other SNe Ia. The light curves are much broader than those of spectroscopically normal SNe Ia such as SN 2005cf. Even in comparison to the overluminous SN 1991T, SN 2009dc evolves significantly more slowly. The light curve of SN 2006gz presented by Hicken et al. (2007) provides a good match, although SN 2009dc appears to have a slower rise time *and* a slower decline.

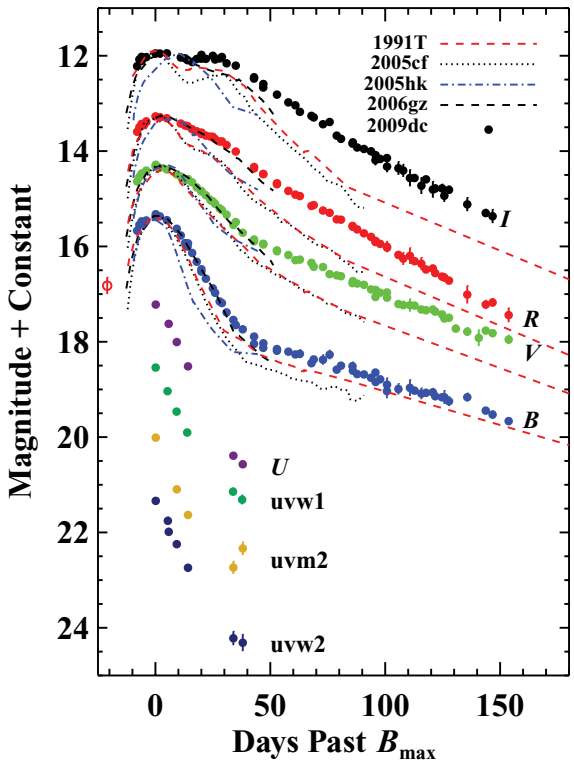

Figure 2. Optical and ultraviolet (UV) light curves of SN 2009dc from KAIT and the 1-m Lick Nickel telescope. For comparison we also plot the optical light curves of the overluminous Type Ia SN 1991T, the normal SN 2005cf, the peculiar SN 2002cx-like SN 2005hk and another SC SN Ia candidate SN 2006gz. The light curves of each SN are shifted so that $t = 0$ d corresponds to the time of B_{max} and reach the same peak magnitude for a given filter. The evolution of SN 2009dc is atypical compared to other SNe Ia. SN 2009dc evolves much more slowly and exhibits only a muted secondary maximum in the *I* band. We include in our *R*-band light curve an early detection of SN 2009dc (red open circle) in an unfiltered image from the Lick Observatory SN Search (LOSS), about 3 weeks before maximum brightness. The data sources for the other SNe are cited in the text.

The absence of a prominent second maximum in the *R* and *I* bands is particularly striking. The secondary maximum in *I* has been attributed to the propagation of an ionization front through IGEs as they transition from being doubly ionized to singly ionized (Kasen 2006). Observationally, the strength of the secondary maximum has been found to correlate with peak luminosity, powered by Ni decay, with luminous SNe exhibiting more prominent secondary peaks (Hamuy et al. 1996; Nobili et al. 2005). However, this feature is weak in SN 2009dc, even though it is more luminous than a typical SN Ia. Kasen (2006) found that significant mixing of ^{56}Ni in the composition of a SN Ia can lead to a blending of the two *I*-band peaks, possibly explaining why a secondary peak is weak in SN 2009dc.

After correcting for Milky Way (MW) extinction (from the dust maps of Schlegel, Finkbeiner & Davis 1998), we fit a polynomial to the *B*-band light curve to find that SN 2009dc peaked on JD 245 4946.93 ± 0.2 (on 2009 Apr. 25.4) at $B_{max} = 15.05 \pm 0.04$ mag. These values are consistent with those derived by Yamanaka et al. (2009).

We also measure $\Delta m_{15}(B)$, the decline in flux from maximum light to 15 d past maximum in the *B* band. Correcting for time dilation, we find $\Delta m_{15}(B) = 0.72 \pm 0.03$ mag, making SN 2009dc one of the most slowly evolving SNe ever discovered and comparable to other SC SN Ia candidates in the literature. Interestingly, Yamanaka et al. (2009) measure $\Delta m_{15}(B) = 0.65 \pm 0.03$ mag. Comparing the two photometric data sets, we find discrepancies between measurements of local standard stars of ∼0.15 mag. With over 10 calibrations of the field on photometric nights, we are confident in our measurements of the field standards presented in Table 1. While these differences are troubling, they do not alter the conclusion that SN 2009dc is a slowly evolving SN with an extreme value of $\Delta m_{15}(B)$.

The host galaxy of SN 2009dc is part of the LOSS (Li et al. 2000; Filippenko et al. 2001), allowing us to put strict constraints on the rise time of SN 2009dc. Our first detection of SN 2009dc is from an unfiltered image on 2009 Apr. 4, when the SN is seen at $R = 18.82 \pm 0.18$ mag, indicating a rise time >21 d. This first detection is included in Fig. 2 as part of our *R*-band data [Li et al. (2003a) show that KAIT unfiltered data approximate the *R* band]. In an image taken on 2009 Mar. 28, there is no detection of SN 2009dc down to $R \approx 19.3$ mag. With these constraints we conservatively estimate a rise time of 23 ± 2 d. Hayden et al. (2010) recently found an average SN Ia rise time of 17.38 ± 0.17 d using 105 SDSS-II SNe Ia, with slowly declining SNe tending to have shorter rise times. The rise time of SN 2009dc is significantly longer than the average SN Ia in their sample, despite being a slowly declining SN, and therefore does not follow the trend found for normal SNe Ia in their sample. Riess et al. (1999), on the other hand, found an average rise time of 19.5 ± 0.2 d for a 'typical' SN Ia [$\Delta m_{15}(B) = 1.1$ mag], with slowly declining SNe having slower rise times. Their sample of 10 objects lacks SNe Ia with $\Delta m(15)_B < 0.95$ mag, making an extrapolation to $\Delta m_{15}(B) = 0.72$ mag to compare with the rise time of SN 2009dc unreliable.

The cosmological application of SNe Ia as precise distance indicators relies on being able to standardize their luminosity. Phillips (1993) showed that $\Delta m_{15}(B)$ is well correlated with luminosity at peak brightness for most SNe Ia, the so-called 'Phillips relation'.

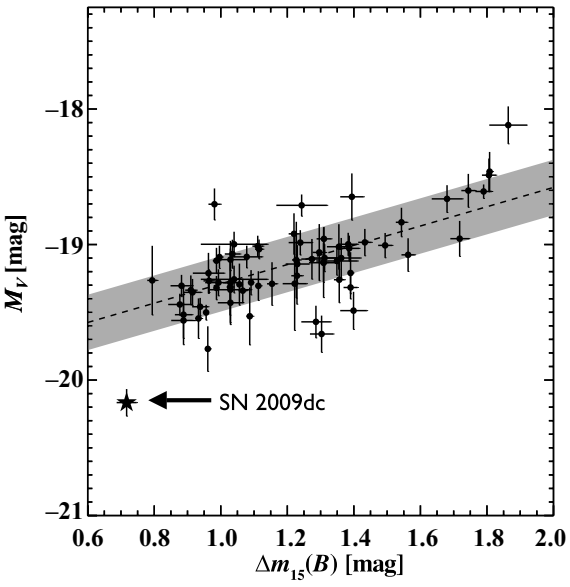

Figure 3. M_V as a function of $\Delta m_{15}(B)$ for 71 SNe Ia with $z_{\rm Virgoinfall} > 0.01$ from the LOSS photometry archive (filled circles, Ganeshalingam et al. in preparation), compared with SN 2009dc (filled star). Host-galaxy extinction is derived using MLCS2k2.v006 (Jha et al. 2007), except in the case of SN 2009dc where we adopt $E(B-V)_{\rm host} = 0.1$ mag with $R_V = 3.1$ (see Section 3.5 for details). The luminosity distance was calculated using the ΛCDM concordant cosmology with $H_0 = 70\,{\rm km\,s^{-1}\,Mpc^{-1}}$, $\Omega_{\rm m} = 0.27$ and $\Omega_\Lambda = 0.73$ (Spergel et al. 2007). The best-fitting line to the data, excluding SN 2009dc, in the range $0.6 < \Delta m_{15}(B) < 1.7$ mag, is plotted as a dashed line, with points that fall within 1σ shaded in grey. SN 2009dc is clearly an outlier that does not follow the luminosity–width relation.

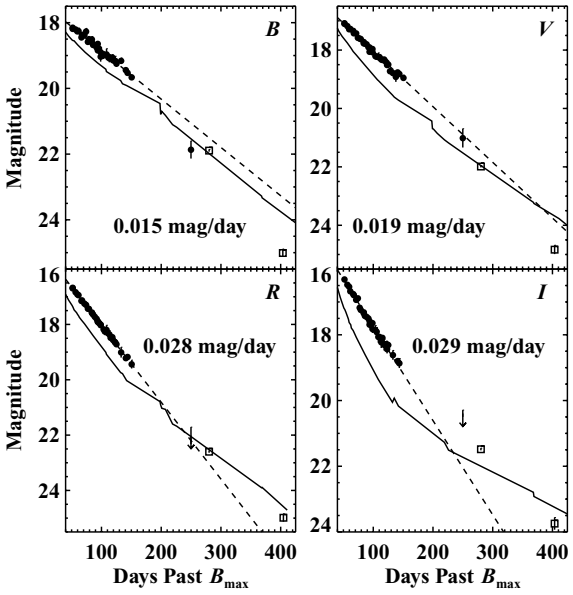

Figure 4. The late-time decay of SN 2009dc from 50 to about 400 d past maximum light compared to that of SN 2003du (solid line), a typical SN Ia. The light curves are shifted such that $t = 0$ d corresponds to the time of $B_{\rm max}$, and a constant has been added to each SN 2003du light curve to match the peak magnitude of SN 2009dc. Filled circles are KAIT and Nickel data, whereas open squares are LRIS and DEIMOS data. Upper limits are marked with arrows. The LRIS g-band point is plotted in the B-band light curve panel. We fit the decay in $BVRI$, plotted as a dashed line, using a linear least-squares fit to our well-sampled data between 50 and 150 d past maximum, before the SN became projected too close to the Sun. Late-time photometry obtained with LRIS at 281 d past maximum indicates that the flux in B and V is below what is expected from linear extrapolations, but mostly agrees with expectations from SN 2003du. However, the flux in R and I is larger than what is expected compared to the extrapolations. Our R-band detection falls on the comparison light curve, while the I-band detection is brighter than what is expected. SN 2009dc is detected in all bands at ∼400 d past maximum, indicating that the SN is still active despite the points lying below interpolated values from SN 2003du. The data for SN 2003du were taken from Stanishev et al. (2007).

In Fig. 3, we plot absolute V magnitude as a function of $\Delta m_{15}(B)$ for 71 SNe Ia with $z_{\rm Virgoinfall} > 0.01$ from the LOSS photometry data base (Ganeshalingam et al. in preparation) and SN 2009dc to determine whether SN 2009dc follows the Phillips relation. Host-galaxy extinction for the sample of 71 SNe Ia is derived using MLCS2k2.v006 with the *glosz* prior, which assumes that the late-time $(B-V)_{t=+35{\rm d}}$ colour is indicative of the host-galaxy extinction (Jha, Riess & Kirshner 2007). For SN 2009dc, the late-time colour evolution differs significantly from that of normal SNe Ia; thus, we instead adopt $E(B-V)_{\rm host} = 0.1$ mag, assuming $R_V = 3.1$ for the host galaxy (see Section 3.5 for details). To place the SNe on an absolute scale, we use the luminosity distance assuming a Λ cold dark matter (ΛCDM) cosmology with $H_0 = 70\,{\rm km\,s^{-1}\,Mpc^{-1}}$. The best-fitting line to SNe with $0.6 < \Delta m_{15}(B) < 1.7$ mag, excluding SN 2009dc, is plotted in Fig. 3, with the area that falls within 1σ of the relation shaded in grey. SN 2009dc is clearly an overluminous outlier in comparison to SNe Ia having similar values of $\Delta m_{15}(B)$. Events similar to SN 2009dc cannot be standardized using current distance-fitting techniques which rely on parametrizations of light-curve shape (Howell et al. 2006).

We measure the late-time decay of the light curves using a linear least-squares fit to data in the range ∼50–150 d after maximum. We find a decline of 1.47 ± 0.04 mag per 100 d in B, 1.91 ± 0.02 mag per 100 d in V, 2.78 ± 0.03 mag per 100 d in R and 2.87 ± 0.04 mag per 100 d in I. Leibundgut (2000) find typical decay rates for SNe Ia of 1.4 mag per 100 d in B, 2.8 mag per 100 d in V and 4.2 mag per 100 d in I. SN 2009dc shows significantly slower decline rates in V and I.

Late-time photometry of SN 2009dc (Table 3) taken with the Nickel telescope shows only marginal detections in B and V and upper limits in R and I, while our Keck images, 281 d past maximum, give clear detections in $gVRI$. Fig. 4 shows the late-time behaviour of SN 2009dc in comparison to late-time photometry of SN 2003du, a typical SN Ia, taken from Stanishev et al. (2007), and the linear decay rates found using data ∼50–150 d after maximum. A constant has been added to each SN 2003du light curve in order to match the peak magnitude of SN 2009dc. Compared to the extrapolations based on the measured linear decay rates, at 281 d past maximum SN 2009dc is fainter by ∼0.5 mag in B and V, brighter by ∼0.5 mag in R and ∼1.5 mag brighter in I. In comparison to SN 2003du, SN 2009dc is within ∼0.15 mag of the interpolated values in BVR and ∼0.5 mag brighter in I. We caution that our interpolated values for SN 2003du suffer from a rather large gap in the light curve between 225 and 366 d after maximum. While the late-time behaviour of SN 2009dc does not match the linear decay of SN 2003du exactly in all bands, our detections indicate that it has not undergone an unexpected drop in luminosity, and it is consistent with the late-time light curve being powered by ^{56}Co decay (see Section 4.2).

The data taken ∼400 d past maximum show only marginal detections in all bands, indicating that the SN is still active despite the points lying below interpolated values from SN 2003du. The detections in B and V are clearly below what we would expect from

SN 2003du, while R and I are not too far below expectations. We address possible reasons for the drop in flux in Section 4.2.2.

3.2 Colour evolution

The colour evolution in $B - V$, $V - R$ and $R - I$ for SN 2009dc in comparison to SNe 2006gz, 2005cf, 1991T and 2005hk is displayed in Fig. 5. All SNe have been corrected for MW extinction using reddening derived from the dust maps of Schlegel et al. (1998). We have also corrected for host-galaxy extinction, assuming $R_V = 3.1$, using the following reported values of $E(B - V)_{\rm host}$: 0.13 mag for SN 1991T (Lira et al. 1998), 0.10 mag for SN 2005cf (Wang et al. 2009b), 0.09 mag for SN 2005hk (Phillips et al. 2007), 0.18 mag for SN 2006gz (Hicken et al. 2007) and 0.10 mag for SN 2009dc.

The colour curves indicate that SN 2009dc was a particularly blue SN Ia even compared to the prototypical overluminous SN 1991T. In $B - V$, SN 2009dc remains bluer than SNe 1991T, 2005cf and 2005hk until ∼50 d past maximum light. The colour curves for SN 2009dc are most similar to those of SN 2006gz, another SC SN Ia candidate. At $t > 50$ d, the $B - V$ colour of SN 2009dc becomes redder than that of SN 1991T and SN 2005cf.

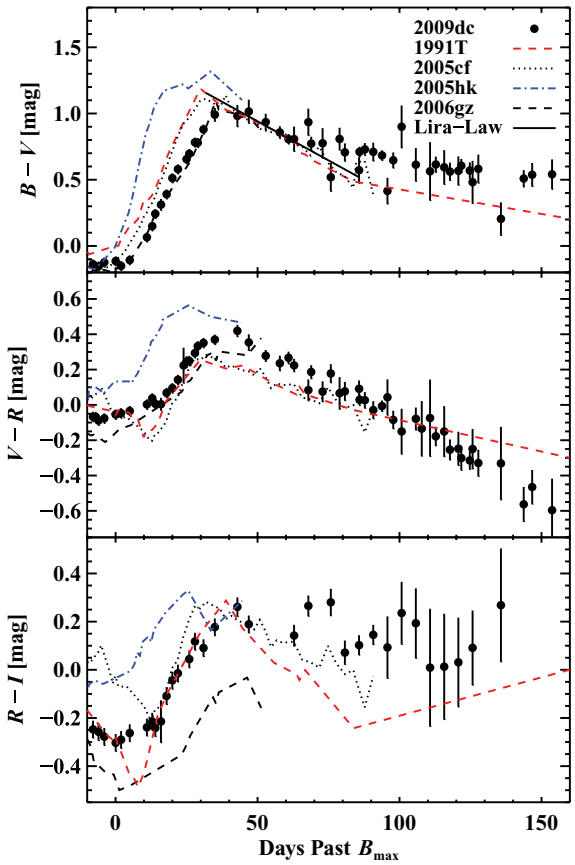

Figure 5. $B - V$ (top), $V - R$ (middle) and $R - I$ (bottom) colour curves of SN 2009dc. Plotted for comparison are the colour curves of SNe 1991T, 2005cf, 2005hk and 2006gz. All curves have been corrected for MW reddening and host-galaxy extinction. We have not included errors in derived host-galaxy extinction for SN 2009dc which will systematically shift curves in one direction. At early times, SN 2009dc is bluer than SNe 1991T, 2005cf and 2005hk. The evolution most clearly resembles that of SN 2006gz. We plot the Lira law as a solid line in the range $35 < t < 85$ d. SN 2009dc shows a slower red to blue colour evolution compared to the Lira–Phillips relation, especially after $t = 70$ d. The data sources are cited in the text.

Lira (1996) showed that SNe with low host-galaxy extinction had similar $B - V$ colour evolution between $t = +30$ to $+90$ d independent of light-curve shape (the 'Lira–Phillips relation'). Hicken et al. (2007) used this relationship to derive the host-galaxy extinction for SN 2006gz. However, a comparison between the slope of the Lira–Phillips relation and the $B - V$ colour evolution of SN 2009dc shows disagreement. Adopting the relation derived using six low-reddening SNe Ia by Phillips et al. (1999) and fitting for a constant $E(B - V)_{\rm host}$ between $t = +35$ and $+90$ d, we find $E(B - V)_{\rm host} = 0.26 \pm 0.04$ mag, with $\chi^2 = 41$ for 15 degrees of freedom. If we restrict our fit to between $t = +35$ and $+70$ d, we find a better fit with $E(B - V)_{\rm host} = 0.19 \pm 0.04$ mag; $\chi^2 = 5$ for 7 degrees of freedom. We include the fit to the Lira–Phillips relation in Fig. 5.

3.3 Pre-maximum spectrum

On 2009 Apr. 16.22, ∼9 days before B-band maximum, Harutyunyan et al. (2009) obtained a spectrum of SN 2009dc which showed 'prominent C II lines and a blue continuum', and they noted that the spectrum resembled pre-maximum spectra of SN 2006gz (Hicken et al. 2007), but with a much lower expansion velocity. We obtained a spectrum ∼2 days later which confirmed the spectral peculiarities noted by Harutyunyan et al. (2009).

Our pre-maximum spectrum is shown in Fig. 6, where we compare SN 2009dc to other possible SC SNe Ia: SN 2006gz (Hicken et al. 2007), SN 2003fg (Howell et al. 2006) and SN 2004gu (Contreras et al. 2010, though the displayed spectrum is from our own data base). In addition, we show for comparison spectra from similar epochs of the 'standard overluminous' Type Ia SN 1991T (Filippenko et al. 1992), the SN 2002cx-like peculiar SN 2005hk (Chornock et al. 2006) and the 'standard normal' Type Ia SN 2005cf (Wang et al. 2009b).

SN 2009dc has strong Si II and S II lines, and appears to also contain O I, all of which are usually found in near-maximum spectra of SNe Ia. However, there are also two apparent C II lines (labelled in Fig. 6 and discussed in Section 3.3.2) seen in SN 2009dc. The existence (and strength) of these features is one reason that SN 2009dc was immediately classified as a possible SC SN Ia (Harutyunyan et al. 2009), and one way used to distinguish it from other subtypes of SNe Ia.

Spectroscopically, SN 2009dc does not seem to resemble any of SNe 1991T, 2005hk or 2005cf. Although SN 2006gz has weak C II features at 14 d before maximum, by 8 d before maximum they have almost completely disappeared (whereas SN 2009dc has strong C II at 7 d before maximum). In addition, it is apparent from Fig. 6 that the expansion velocity of SN 2006gz is much larger than that of SN 2009dc (based on the Si II λ6355 feature, for example; see Section 3.3.1 for further details). Finally, SN 2003fg does seem to resemble SN 2009dc, even though the spectrum of SN 2003fg has low signal-to-noise ratio (S/N) and the C II features are not nearly as prominent in SN 2003fg as they are in SN 2009dc. It is possible that this is due to the fact that the spectrum of SN 2003fg was taken 9 d later (relative to maximum light) than our spectrum of SN 2009dc.

3.3.1 Si II

The tell-tale spectroscopic signature of a SN Ia is broad absorption from Si II λ6355 (e.g. Filippenko 1997), and SN 2009dc is no different. One thing that *is* interesting about the Si II feature in SN 2009dc is its extremely low velocity. The minimum of the Si II λ6355 absorption feature was found to be blueshifted by 8700 km s^{-1} about

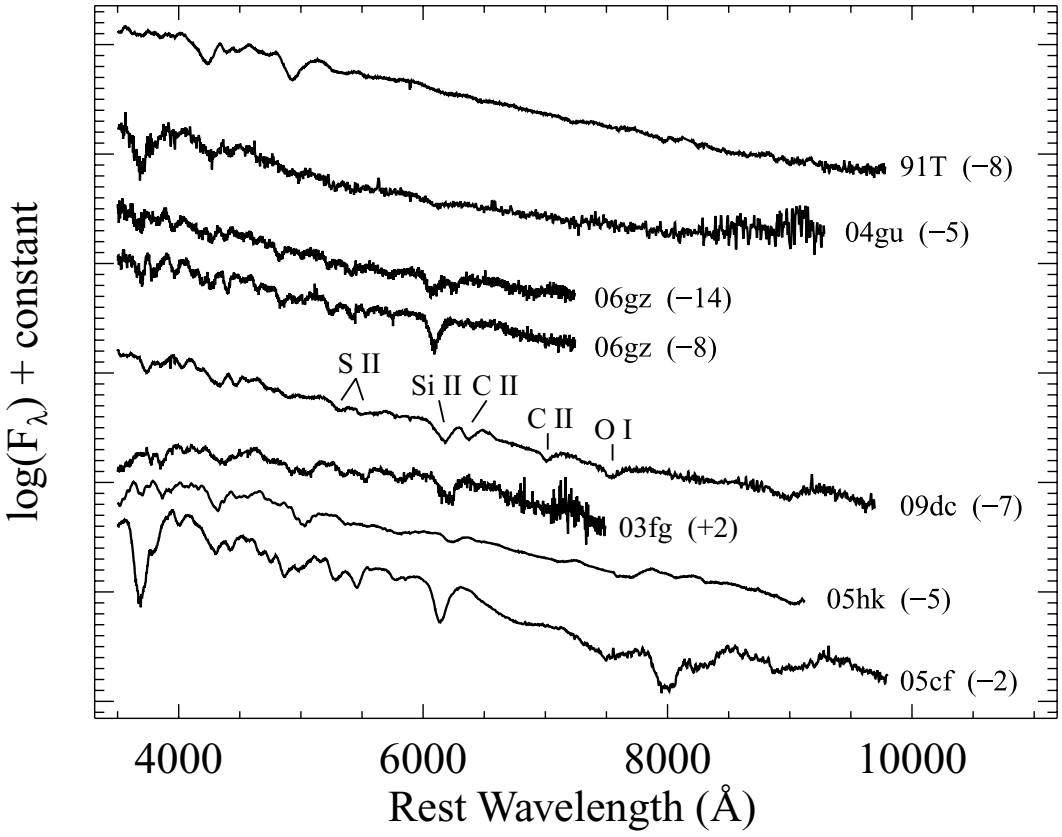

Figure 6. Our pre-maximum spectrum of SN 2009dc (and various comparison SNe) with a few major lines identified and days relative to maximum light indicated for each spectrum (in parentheses). From top to bottom, the SNe are the 'standard overluminous' Type Ia SN 1991T (Filippenko et al. 1992), a possible SC SN Ia SN 2004gu (Contreras et al. 2010, though this spectrum is from our own data base), another possible SC SN Ia SN 2006gz (Hicken et al. 2007) at two different epochs, SN 2009dc (this work), yet another possible SC SN Ia SN 2003fg (Howell et al. 2006), the SN 2002cx-like peculiar SN 2005hk (Chornock et al. 2006) and finally the 'standard normal' Type Ia SN 2005cf (Wang et al. 2009b). All spectra have had their host-galaxy recession velocities removed and have been dereddened according to the values presented in their respective references. Note that Si II, S II and O I are often found in near-maximum spectra of SNe Ia, but C II is not.

9 d before maximum brightness (Harutyunyan et al. 2009), and we measure the feature to be blueshifted by ∼8600 km s^{-1} in our spectrum taken 7 d before maximum. Yamanaka et al. (2009) report it to be blueshifted by 8000 km s^{-1} in their spectrum 3 d before maximum, decreasing to 6000 km s^{-1} by 25 d after maximum.

These velocities are much lower than the average photospheric velocity near maximum for SNe Ia of ∼11 000 km s^{-1} (Wang et al. 2009a). In fact, according to Wang et al. (2009a), the Si II velocities seen in SN 2009dc are approximately 8σ below the average.[2]

Interestingly, these velocities *are* similar to those of two other possible SC SNe Ia, SN 2003fg and SN 2007if, respectively (Howell et al. 2006; Scalzo et al. 2010). However, two other objects that were claimed to be possible SC SNe Ia show much more normal Si II velocities. Hicken et al. (2007) report expansion velocities near maximum light of about 11 000–13 000 km s^{-1} for SN 2006gz. SN 2004gu, which was compared to SN 2006gz by Contreras et al. (2010), also shows a normal photospheric velocity of ∼11 500 km s^{-1} at 5 d before maximum (this work) slowing to ∼11 000 km s^{-1} at 3 d past maximum.[3]

Fig. 4 of Yamanaka et al. (2009) and fig. 4 of Scalzo et al. (2010) both present the velocity evolution of the Si II λ6355 feature for various possible SC SNe Ia and other comparison SNe. Our new early-time data point (i.e. ∼8600 km s^{-1} at $t \approx -7$ d) is quite consistent with the rest of the published SN 2009dc data. Moreover, we detect Si II λ6355 in our next spectrum taken 35 d past maximum at a blueshifted velocity of about 5500 km s^{-1} (see Section 3.4.1 for further details). This yields a velocity gradient of ∼74 km s^{-1} d^{-1}, which is over twice as large as that found for SN 2007if (34 km s^{-1} d^{-1}; Scalzo et al. 2010). Furthermore, combining our measurements with all previously published values of the expansion velocity of SN 2009dc (Harutyunyan et al. 2009; Yamanaka et al. 2009; Tanaka et al. 2010), we see no strong evidence for a velocity 'plateau' near maximum light like the one seen in SN 2007if (Scalzo et al. 2010).

We measure the equivalent width (EW) of the Si II λ6355 feature to be ∼40 Å in our spectrum of SN 2009dc obtained 7 d before

[2] Note that they consider SNe Ia with photospheric velocities greater than 3σ above the average to be 'high-velocity SNe Ia'.

[3] This second velocity has a large uncertainty since it was measured by approximating the minimum of the Si II absorption feature by eye from fig. 3 of Contreras et al. (2010).

maximum. This is similar to the EW of the same line in SN 2006gz at similar epochs (Hicken et al. 2007), and both are well below the average Si II EW for normal SNe Ia (though they are comparable to the overluminous SN 1991T-like SNe Ia; e.g. Hachinger, Mazzali & Benetti 2006; Wang et al. 2009a).

3.3.2 C II

As ubiquitous as Si II is in the spectra of SNe Ia, C II is nearly as rare. In a few cases, mainly at very early times, weak C II has been detected in optical spectra of SNe Ia (e.g. Branch et al. 2003; Thomas et al. 2007; Tanaka et al. 2008; Foley et al. 2010). Candidate SC SNe Ia, on the other hand, exhibit strong C II in their near-maximum spectra (Howell et al. 2006; Hicken et al. 2007; Scalzo et al. 2010).

In our spectrum of SN 2009dc obtained 7 d before maximum brightness, we detect absorption from C II λ6580 and λ7234 (both of which were also detected in a spectrum obtained the same day by Marion et al. 2009). The minimum of the absorption from C II λ6580 is blueshifted by about 9500 km s^{-1} in our pre-maximum spectrum. The expansion velocity of this feature is ∼8500 km s^{-1} at 3 d before maximum, slowing to about 7000 km s^{-1} at 3 d after maximum, and ∼6700 km s^{-1} by 6 d after maximum (Yamanaka et al. 2009; Tanaka et al. 2010). By about 18 d past maximum, this feature seems to have completely disappeared, though it is difficult to be sure given the low S/N spectrum seen in fig. 3 of Yamanaka et al. (2009). However, it is clear from the same figure that by 25 d after maximum, the feature is most definitely gone. It is also undetected in our spectrum obtained 35 d past maximum (see Section 3.4).

Also, from our pre-maximum spectrum of SN 2009dc, we measure the minimum of the C II λ7234 absorption to be ∼9400 km s^{-1}, which is in good agreement with the velocity of the C II λ6580 feature that we calculate above. This feature is still apparent at about 6 d past maximum, near a velocity of ∼6600 km s^{-1} (see fig. 1 of Tanaka et al. 2010, though the feature is not marked), but it has also likely disappeared by 18 d past maximum (Yamanaka et al. 2009, Fig. 3) and is certainly gone by 35 d past maximum (see Section 3.4).

For C II, the velocities seen in SN 2009dc once again match those of SN 2003fg at ∼2 days past maximum (Howell et al. 2006, Fig. 3 and Supplementary Information), though only the C II λ4267 line (at an expansion velocity of ∼8300 km s^{-1}) is clearly detected. On the other hand, SN 2007if appears to have both the C II λ6580 and λ7234 features in its spectrum from 5 d past maximum (Scalzo et al. 2010).

A spectrum of SN 2006gz at 13 d before maximum shows both the C II λ6580 and C II λ7234 lines with expansion velocities near 15 500 km s^{-1}. However, both features are effectively undetectable 4 d later (Hicken et al. 2007). We also note that neither line is seen in spectra of SN 2004gu at 5 d before maximum (see Fig. 6, although this spectrum has low S/N) or at 3 d after maximum (Contreras et al. 2010).[4]

For SN 2009dc, Marion et al. (2009) reported no detectable absorption from C II λ4745 in their spectrum obtained 7 d before maximum. However, in our spectrum taken on the same day, we *do* see evidence for absorption from this transition, as well as absorption from C II λ4267 (see Section 3.3.4). Note that both of these features are slightly blended with absorption from other species, which is what most likely led Marion et al. (2009) to conclude that the features were not present.

The EW of the C II λ6580 and λ7234 absorptions, as calculated from our spectrum taken 7 d before maximum, is ∼19 and ∼13 Å, respectively. Hicken et al. (2007) report that the C II λ6580 feature in SN 2006gz 14 d before maximum had an EW that was slightly higher than these values (25 Å). Both of these SNe have much stronger C II lines than typical SNe Ia. For example, one of the strongest C II features ever seen in a normal SN Ia was in SN 2006D, where C II λ6580 was detected with an EW of merely 7 Å (Thomas et al. 2007).

3.3.3 Ca II

In our pre-maximum spectrum (as well as most of our post-maximum spectra; see Section 3.4) we detect narrow, as well as broad, absorption from Ca II H&K. The narrow components are at the redshift of SN 2009dc and its host galaxy. At all epochs these lines are just at our instrumental resolution limit; thus, calculating an accurate FWHM is nearly impossible. In addition, the H&K lines occur in a part of the spectrum where numerous broad absorption features blend together, so defining a local continuum is difficult, exacerbating the problem of measuring reliable line strengths. Despite all this, we attempt to measure the strength of this narrow feature. We calculate that the Ca II H&K lines appear to have FWHM ranging from about 100–300 km s^{-1}. However, the line strengths are consistent with no change during these epochs, given our rather large uncertainties.

Some SNe Ia exhibit narrow, time-variable Na I D absorption lines with unchanging, narrow Ca II H&K absorption (e.g. Simon et al. 2009). However, time-variable Ca II H&K absorption has not been seen. SN 2009dc does show weak, narrow absorption from Na I D, but it is far too weak to determine if variability in the line strengths exists (see Section 3.5). We cannot claim to have detected narrow, time-variable Ca II H&K absorption in SN 2009dc, but such variability should be searched for in other, future SC SNe Ia.

The narrow Ca II H&K may arise from calcium-rich interstellar material (ISM) in the host galaxy of SN 2009dc, UGC 10064, and in fact this feature is strong in a spectrum of the core of the galaxy (Abazajian et al. 2009). However, since SN 2009dc is relatively far from the host's nucleus, this seems somewhat unlikely. The alternative is that the calcium-rich material which gives rise to the strong Ca II H&K line is in close proximity to the SN site. This means that SN 2009dc likely exploded in a region of calcium-rich ISM, or that the progenitor star of SN 2009dc itself had calcium-rich circumstellar material. However, which of these two possibilities best reflects the true situation and how this may affect the SN itself are beyond the scope of this paper.

Another Ca II feature commonly seen in SNe Ia is the broad Ca II near-IR triplet. However, we see no hint of this line in our spectrum obtained 7 d before maximum. On the other hand, Tanaka et al. (2010) clearly detect this feature near 8400 Å in their spectropolarimetric observations taken ∼6 days after maximum. Not only is the line apparent in their total-flux spectrum, but it is the most polarized spectral feature they detect, with a total polarization of ∼0.7 per cent. This, along with the high polarization of Si II λ6355 and the relatively low continuum polarization led Tanaka et al. (2010) to conclude that SN 2009dc had a roughly spherical photosphere (as is the case for most normal SNe Ia; e.g. Leonard et al. 2005; Chornock & Filippenko 2008) with a somewhat clumpy distribution of intermediate-mass elements (IMEs).

[4] The C II λ7234 line, if present, would be at the red end of this spectrum.

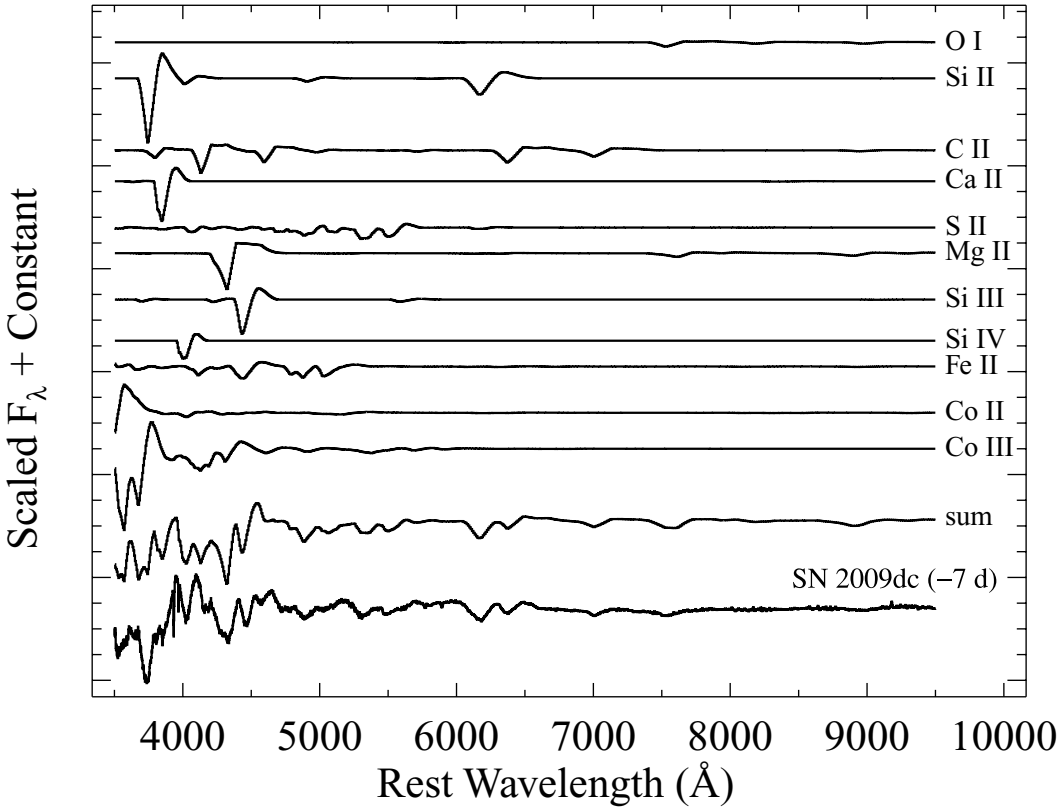

Figure 7. The top 11 spectra show the constituent species in our SYNOW fit. The second from bottom spectrum is the sum of the top 11 spectra. The bottom spectrum is our pre-maximum spectrum of SN 2009dc [dereddened by $E(B-V)_{\rm MW} = 0.070$ mag and $E(B-V)_{\rm host} = 0.1$ mag with $R_V = 3.1$]. We also remove the host-galaxy recession velocity ($cz = 6300 \pm 300$ km s^{-1}). Finally, we remove the underlying 20 000 K blackbody continuum from all spectra shown.

3.3.4 Other species and the synow *fit*

To determine which other species are present in our pre-maximum spectrum of SN 2009dc, we use the spectrum-synthesis code SYNOW (Fisher et al. 1997). SYNOW is a parametrized resonance-scattering code which allows for the adjustment of optical depths, temperatures and velocities in order to help identify spectral features seen in SNe.

Before fitting, we deredden our pre-maximum spectrum of SN 2009dc using $E(B-V)_{\rm MW} = 0.070$ mag, $E(B-V)_{\rm host} = 0.1$ mag (see Section 3.5 for more information on how we derive these values), $R_V = 3.1$ and the reddening curve of Cardelli, Clayton & Mathis (1989). We also remove the host-galaxy recession velocity ($cz = 6300 \pm 300$ km s^{-1}, as determined from the narrow Ca II H&K absorption in our spectrum) before comparing with the output of SYNOW.

Our derived SYNOW fit is compared to our actual pre-maximum spectrum in Fig. 7. Also shown are the spectral features from each of the individual species that were used in the final fit. Our SYNOW fit faithfully reproduces the vast majority of the features seen in our pre-maximum spectrum of SN 2009dc, but a few features are not matched exactly (specifically, the ones near 3700 Å, 4100 Å and 4600 Å).

In addition to the species mentioned above (Si II, C II and weak Ca II), we detect O I, S II, Mg II, Si III, Si IV, Fe II, Co II and Co III. All of these ions (except C II, as mentioned previously) are often found in early-time spectra of SNe Ia, though O I may be weak in some overluminous SNe Ia (e.g. Filippenko 1997). The detection of C II in the spectra of SN 2009dc (see Section 3.3.2) implies that it had a significant amount of unburned material in its ejecta, and thus the oxygen seen in SN 2009dc is most likely from this unburned material as well.

Our SYNOW fit has a photospheric velocity of 9000 km s^{-1}, with maximum velocities of 10 000–15 000 km s^{-1} depending on the ion. This value matches our derived velocities from the Si II and C II absorption features (see Sections 3.3.1 and 3.3.2, respectively). Since the early-time spectra of SN 2009dc and SN 2003fg greatly resemble each other, it is not surprising that these parameters are similar to those found in a SYNOW fit of SN 2003fg (Howell et al. 2006, Supplementary Information). Our fit requires a slightly higher photospheric velocity (they use 8000 km s^{-1}), but this seems reasonable since our spectrum was obtained 7 d *before* maximum and the spectrum of SN 2003fg fit by Howell et al. (2006) is from ∼2 days *after* maximum.

All ions in our SYNOW fit had an excitation temperature around 10 000 K except C II, which was raised to 20 000 K in order to get the relative line strengths to match the data. This is lower than what was calculated by Howell et al. (2006) for SN 2003fg. They required an excitation temperature for C II of 35 000 K to match their spectrum, while we obtain a temperature that is less than 60 per cent of that value.

Finally, we require an underlying blackbody temperature of 20 000 K in order to reproduce the overall continuum shape of SN 2009dc. This is hot for a SN Ia, even at early times, and is indicative of the production of a large amount of ^{56}Ni (Nugent et al. 1995). Blackbody temperatures in the range of 10 000–15 000 K seem to be more common for normal SNe Ia (e.g. Patat et al. 1996), with the overluminous Type Ia SN 1991T having temperatures at the high end of that range (Mazzali, Danziger & Turatto 1995).

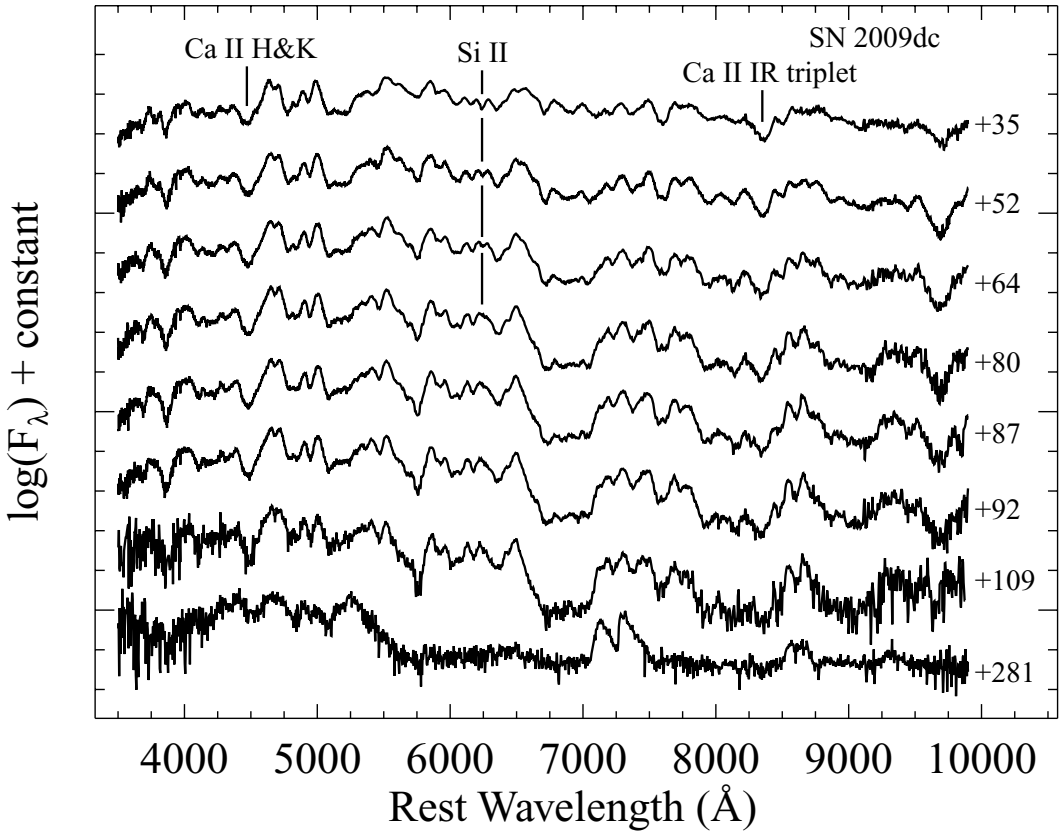

Figure 8. Our post-maximum spectra of SN 2009dc, with days relative to maximum light indicated for each spectrum. Important features discussed in the text are labelled. All spectra have been dereddened by $E(B-V)_{\rm MW} = 0.070$ mag and $E(B-V)_{\rm host} = 0.1$ mag with $R_V = 3.1$. We have also removed the host-galaxy recession velocity ($cz = 6300 \pm 300$ km s^{-1}).

Howell et al. (2006) used a blackbody temperature of 9000 K to fit SN 2003fg, which does not seem abnormally high for a SN Ia 2 d past maximum. Even though this value is a bit lower than our derived blackbody temperature, it is not too surprising since our spectrum of SN 2009dc was obtained about 9 d earlier (relative to maximum light) than their spectrum of SN 2003fg.

3.4 Post-maximum spectra

The rest of our spectral data of SN 2009dc (i.e. all of our post-maximum spectra) are presented in Fig. 8. Note that during our observation on 2009 Aug. 14.2 (day 109), there was smoke and ash in the sky throughout the night (from a fire near the observatory), and thus the continuum shape is less accurate (due to the non-standard extinction caused by the smoke) than in the other observations.

3.4.1 One month after maximum

Our day 35 (2009 May 31.3) spectrum of SN 2009dc is shown in Fig. 9, along with spectra of the peculiar SN 2002cx (Li et al. 2003b), another possible SC SN Ia SN 2007if (Scalzo et al. 2010, though the displayed spectrum is from our own data base) and the 'standard normal' Type Ia SN 2005cf (Wang et al. 2009b). While there are some spectroscopic similarities between SN 2009dc and SN 2005cf at this epoch, there are obvious differences as well. Most notably, there are many more medium-width features in the spectrum of SN 2009dc compared with SN 2005cf, and the features that do clearly match are at much lower velocities in SN 2009dc. This is the same as what was seen in the pre-maximum spectra (Section 3.3). Furthermore, the Ca II H&K feature as well as the Ca II near-IR triplet is much stronger in SN 2005cf than they are in SN 2009dc, again consistent with the pre-maximum spectrum of SN 2009dc (Section 3.3.3).

The possible SC SN Ia SN 2007if appears to be a reasonable match to the spectrum of SN 2009dc, but there are some significant differences. Even though weak Ca II features are detected in both of these objects, there are still a few medium-width features in SN 2009dc that are not seen in SN 2007if. In addition, the velocities of some (but not all) of the features in SN 2007if are larger than those in SN 2009dc by $\sim$1000 km s^{-1}. However, SN 2007if appears to match SN 2005cf well at this epoch, even though its expansion velocity is still not as large as that of SN 2005cf, and SN 2007if is missing the Si II λ6355 absorption seen in SN 2005cf.

The best match to SN 2009dc at this epoch appears to be the peculiar SN 2002cx at an age about 5–10 d younger than SN 2009dc. A detailed discussion of the comparison between peculiar SN 2002cx-like SNe and SN 2009dc can be found in Section 3.4.5. Since nearly every single spectral feature of SN 2009dc at this epoch matches those in SN 2002cx, we use the line identifications of Li et al. (2003b) (which mainly came originally from Mazzali et al. 1997) for SN 2009dc. The spectra at this time are dominated by various multiples of Fe II, although Ca II (as mentioned above), Co II and Na I are also present. There is evidence for O I λ7773 and O I λ9264

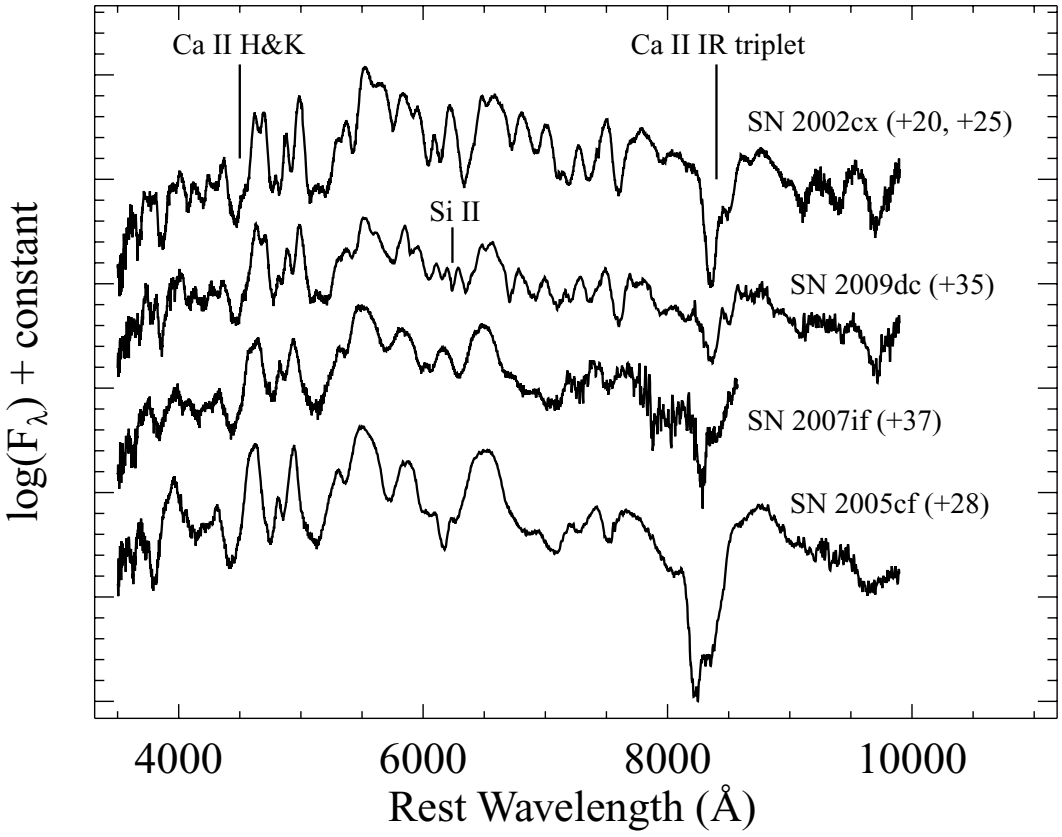

Figure 9. Our spectrum of SN 2009dc 35 d past maximum and a few comparison SNe, with days relative to maximum light indicated for each spectrum (in parentheses). From top to bottom, the SNe are the peculiar SN 2002cx (Li et al. 2003b, where we have combined their spectra from 20 and 25 d past maximum), SN 2009dc (this work), another possible SC SN Ia SN 2007if (Scalzo et al. 2010, though the spectrum shown is from our own data base), and the 'standard normal' Type Ia SN 2005cf (Wang et al. 2009b). Important features discussed in the text are labelled. All spectra have had their host-galaxy recession velocities removed and have been dereddened according to the values presented in their respective references.

(which may give rise to the features seen near 7600 and 9100 Å, respectively), though Branch et al. (2004) claim that a mixture of Fe II and Co II transitions can account for these parts of the spectrum without the need for oxygen. Possible detections of Ti II (Li et al. 2003b) and Cr II (Branch et al. 2004) have been claimed for SN 2002cx, but it is extremely difficult to disentangle the individual contributions of each of these IGEs in SN 2009dc.

The one clear difference between the spectrum of SN 2009dc and that of SN 2002cx (and SN 2005hk as well) is that SN 2009dc has a strong absorption feature centred at 6250 Å that is not seen in either of these other peculiar SNe Ia. This line is also not present in our spectrum of SN 2007if from a similar epoch. In Fig. 10, we present a SYNOW fit to our spectrum of SN 2009dc from 35 d past maximum based originally on a fit to the spectrum of SN 2002cx from 25 d past maximum (Li et al., in preparation). Both SYNOW fits reproduce the majority of the strongest features in SN 2009dc, and the only difference between the two is the addition of Si II at an expansion velocity and excitation temperature similar to other ions in the fit. Based on the comparison of our two fits, we attribute this mysterious absorption in SN 2009dc to Si II λ6355 (blueshifted by ∼5500 km s^{-1}). Note that the spectrum of SN 2005cf from 28 d past maximum, shown in Fig. 9, has strong Si II λ6355 absorption as well. The main difference between these two features is that the absorption in SN 2005cf is blueshifted by ∼9100 km s^{-1}, nearly twice the velocity seen in SN 2009dc. We discuss this feature further in Section 3.4.3.

3.4.2 Two months after maximum

Our day 52 (2009 Jun. 17.5) and day 64 (2009 Jun. 29.3) spectra of SN 2009dc are shown in Fig. 11, along with spectra of SN 2002cx (Li et al. 2003b) and SN 2007if (Scalzo et al. 2010, but the displayed spectrum is from our own data base). Note that SN 2009dc does not evolve much spectroscopically between days 52 and 64, though there are a few differences which will be discussed in Section 3.4.3.

As was the case a month earlier, the spectrum of SN 2009dc at 2 months past maximum matches that of SN 2002cx at a similar epoch. Again, the overall shape and line profiles look extremely similar between these two objects for the most part, and both look similar to SN 2007if as well as SN 2005hk (Phillips et al. 2007). At this epoch there remain a handful of medium-width features in SN 2009dc that are not seen in SN 2007if, and once again the velocities of some features in SN 2007if appear to be larger than those of SN 2009dc by about 1000 km s^{-1}.

As mentioned above, the Si II λ6355 absorption that was seen in our day 35 spectrum is still present in our day 52 and day 64 spectra of SN 2009dc. However, it decreases in strength significantly during these three observations and disappears almost completely by 80 d past maximum (see Section 3.4.3). Another major difference between SN 2009dc and SN 2002cx is that even though the Ca II H&K features are similar in strength, emission from the Ca II near-IR triplet is weaker in SN 2009dc and has a complex profile with

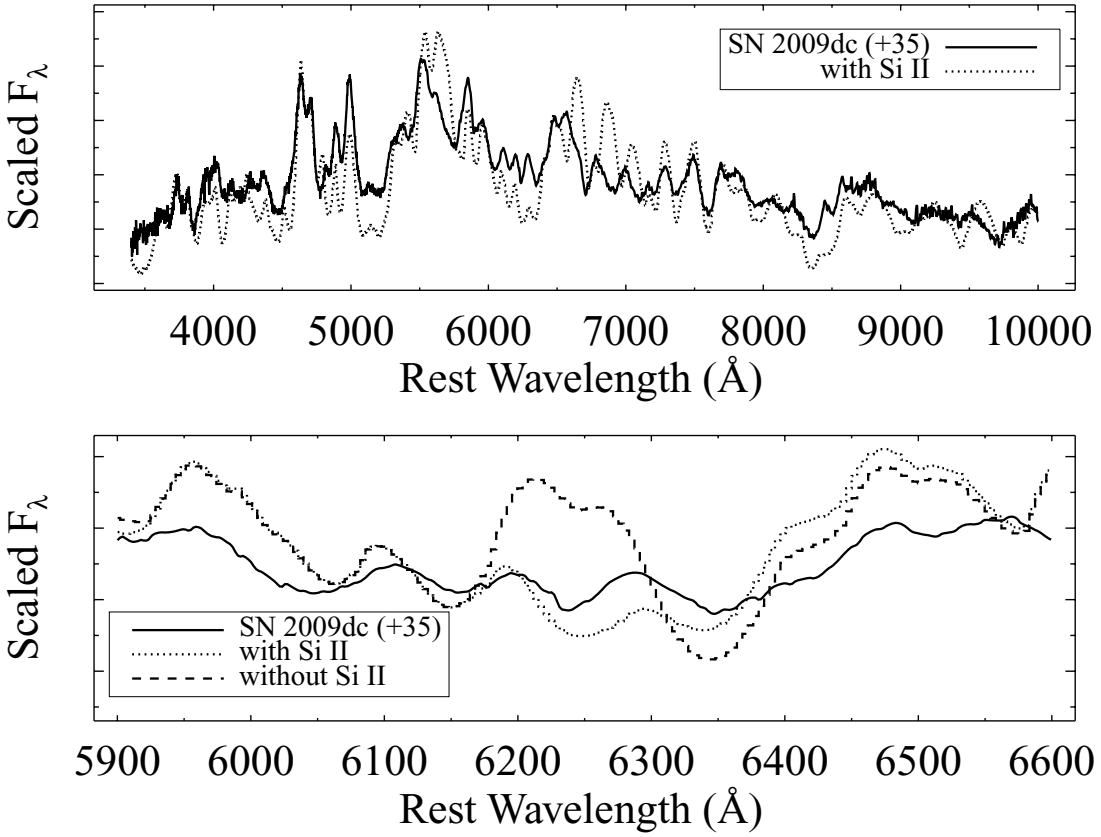

Figure 10. The top panel shows our spectrum of SN 2009dc from 35 d past maximum (solid line) overplotted with our best SYNOW fit which includes Si II (dotted line). The bottom panel is the same as the top panel but zoomed in and centred on the absorption feature in SN 2009dc near 6250 Å; it also shows the same SYNOW fit but with no Si II (dashed line). The SYNOW fit *with* Si II appears to reproduce the data better, and thus we attribute this absorption to Si II λ6355 (blueshifted by ∼5500 km s^{-1}). We have dereddened our data by $E(B-V)_{\rm MW} = 0.070$ mag and $E(B-V)_{\rm host} = 0.1$ mag with $R_V = 3.1$. We have also removed the host-galaxy recession velocity ($cz = 6300 \pm 300$ km s^{-1}) from the data.

multiple peaks. We discuss this feature further in the following section.

3.4.3 Three to four months after maximum

Fig. 8 shows all of our post-maximum spectra of SN 2009dc. Overall, the spectra do not change very much from 35 to 109 d past maximum (see Section 3.4.4 for more information on our spectrum obtained 281 d past maximum). Most of the major spectral features remain constant during these epochs (except for a few notable examples discussed below) and their profile shapes are largely unaltered as well. The profiles of the features that do change with time mainly seem to weaken in a symmetric manner. That is, there is no compelling evidence for a preferential increase or decrease of flux in the blue or red wings of any feature.

One of the most striking aspects of the spectral evolution of SN 2009dc over these epochs is the disappearance of the broad emission near 5400 Å and in the ranges 6500–7200 Å, 7800–8300 Å and (to a lesser extent) 8800–9200 Å. The first two of the ranges mainly fall into the *R* and *I* bands, respectively. The emission from these features, which is strong through about 1 month past maximum and then begins to decrease with time, is possibly responsible for the plateau-like broad peak in the *R* and *I* bands near maximum brightness and their slow late-time decline (as compared to more normal SNe Ia; see Fig. 2).

Li et al. (2003b) also saw these features in SN 2002cx, and their temporal evolution and the effect they had on the near-maximum *R*- and *I*-band light curves are nearly identical to what we find in SN 2009dc. However, Li et al. (2003b) were unable to determine which ions were responsible for some of the features in these ranges in SN 2002cx, and we are likewise unsure of their origin. The detailed spectral modelling required to definitively determine their identity is beyond the scope of this paper.

As noted previously, we detect strong Si II λ6355 absorption in our day 35 spectrum of SN 2009dc. This feature is still present, but weakens, in our spectra from 52 and 64 d past maximum. In our observation of SN 2009dc at 80 d past maximum there remains a hint of absorption from Si II λ6355, but it is almost non-existent and it is effectively undetected in any of our later spectra. It is unusual to see such strong absorption from Si II λ6355 in a SN Ia at such late times. For example, at 46 d past maximum the spectrum of SN 2005cf has only a barely perceptible Si II λ6355 feature (Wang et al. 2009b, fig. 17).

The relative strength of this Si II line at late times in SN 2009dc is possibly due to its large ejecta mass. In Section 4.2, we find that SN 2009dc has one of the largest ^{56}Ni masses ever produced by a SN Ia, and thus one of the largest total ejecta masses as well. The massive ejecta may imply that a greater than average amount of silicon was synthesized in the explosion of SN 2009dc, which could give rise to the rather long-lived Si II λ6355 line that we detect. However, it is also possible that the Si-rich ejecta have an aspherical or clumpy

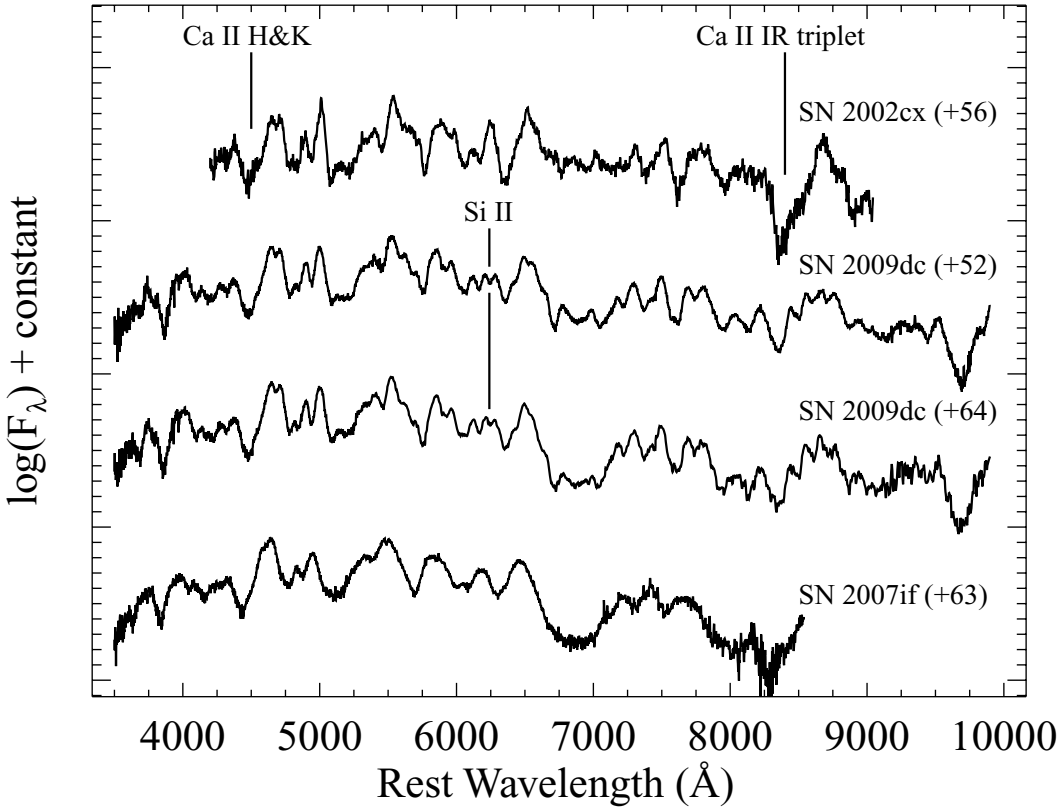

Figure 11. Our spectra of SN 2009dc about 52 and 64 d past maximum, and a few comparison SNe with days relative to maximum light indicated for each spectrum (in parentheses). The top SN is the peculiar SN 2002cx (Li et al. 2003b), the next two spectra are SN 2009dc (this work), and the bottom spectrum is another possible SC SN Ia SN 2007if (Scalzo et al. 2010, though the displayed spectrum is from our own data base). Important features discussed in the text are labelled. All spectra have had their host-galaxy recession velocities removed and have been dereddened according to the values presented in their respective references.

distribution, and thus the longevity of the observed Si II λ6355 line is simply a viewing angle effect.

As stated earlier, another major difference between SN 2009dc and SN 2002cx is that emission from the Ca II near-IR triplet is weaker in SN 2009dc and has a complex profile with multiple peaks, even though the Ca II H&K features are similar in strength. A SYNOW fit indicates that we are actually resolving the individual components of the Ca II near-IR triplet along with shallow absorption possibly from Mg I and another unidentified ion. The Ca II and Mg I features are blueshifted by ∼6000 km s^{-1}, which matches fairly well with our previously calculated post-maximum expansion velocities (see Section 3.4.2). Thus, it seems that the complex structure seen in our post-maximum spectra of SN 2009dc near 8600 Å is a mixture of the Ca II near-IR triplet, Mg I and probably another ion whose identity we are unable to definitively determine.

3.4.4 Nine months after maximum

On 2010 Feb. 6.6 (281 d after maximum), we obtained our final spectrum of SN 2009dc, shown in Fig. 12 along with late-time spectra of the normal Type Ia SN 1998bu (Jha et al. 2006), SN 2006gz (Maeda et al. 2009), another normal Type Ia SN 1990N (Gómez & López 1998, via the online SUSPECT data base[5]) and SN 2002cx (Jha et al. 2006).

[5] http://suspect.nhn.ou.edu/∼suspect

At over 9 months past maximum light, SN 2009dc appears to have completely transitioned to the nebular phase. The SN ejecta are now optically thin and the spectrum shows various emission features. The broad peaks in the range 3800–5500 Å are usually attributed to blends of various features from [Fe II] and [Fe III] (e.g. Mazzali et al. 1998). These blends appear slightly weaker in SN 2009dc as compared to the normal Type Ia SNe 1998bu and 1990N at similar epochs. Interestingly, Maeda et al. (2009) found that SN 2006gz completely lacks these features, though their spectrum has a low S/N.

The Ca II near-IR triplet is detected in both of the normal SNe Ia presented in Fig. 12 as well as in SN 2009dc and possibly SN 2006gz (though the spectrum is noisy at these wavelengths). There is essentially no emission in either SN 2009dc or SN 2006gz from ∼5700 to ∼6800 Å, a region in which [Co III] emission has been identified in normal SNe Ia (Kuchner et al. 1994; Ruiz-Lapuente et al. 1995). The ratio of emission from the strongest [Fe III] feature (4589–4805 Å) to emission from the strongest [Co III] feature (5801–5995 Å) has been measured in a handful of SNe Ia at late times; it increases with both phase relative to maximum and ejecta temperature (Kuchner et al. 1994).

Using our spectra of SNe 1998bu and 1990N shown in Fig. 12, we calculate ratios of about 5.6 and 7.7, respectively. These fit nicely with the other data displayed in fig. 2 of Kuchner et al. (1994). However, it is nearly impossible to calculate this ratio for SN 2009dc and SN 2006gz, since they appear to lack almost any putative cobalt emission at this epoch (and the cobalt and iron

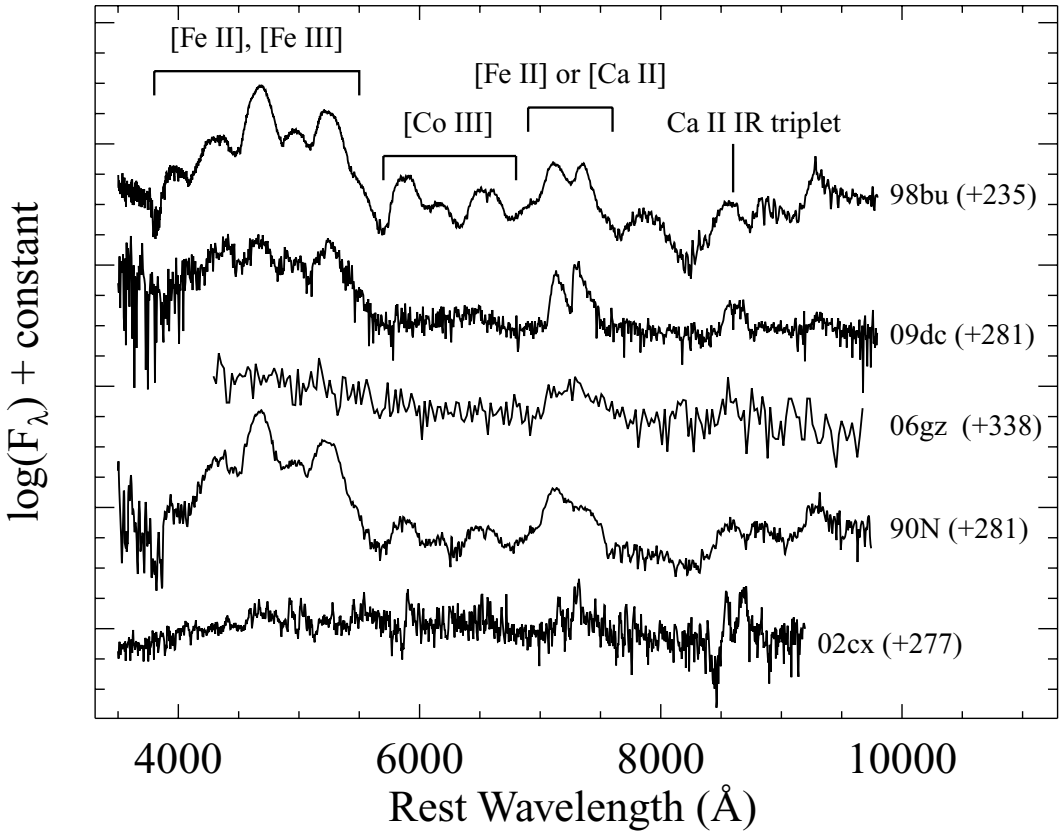

Figure 12. Our spectrum of SN 2009dc about 281 d past maximum, and a few comparison SNe with days relative to maximum light indicated for each spectrum (in parentheses). The spectra from top to bottom are the normal Type Ia SN 1998bu (Jha et al. 2006), SN 2009dc, SN 2006gz (Maeda et al. 2009), SN 1990N (via SUSPECT) and the peculiar Type Ia SN 2002cx (Jha et al. 2006). Major spectral features are labelled. All spectra have had their host-galaxy recession velocities removed and have been dereddened according to the values presented in their respective references.

lines in spectra at earlier epochs are still significantly blended). We attempt to measure the tiny amount of [Co III] emission above the background level from 5801 to 5995 Å and calculate an Fe/Co ratio of about 27. This value, which is likely an underestimate, is already well above that of any other SN Ia at this phase presented by Kuchner et al. (1994). It is also above the dotted lines in fig. 2 of Kuchner et al. (1994), implying that the ejecta temperature of SN 2009dc may be $\gtrsim$10 000 K. Even though this is broadly consistent with our relatively large value of 20 000 K for the blackbody temperature of SN 2009dc before maximum (Section 3.3.4), 10 000 K is extremely hot for a normal SN Ia 9 months past maximum brightness and the shape of the spectrum at this epoch does not seem to support such a high temperature.

The most well-defined spectral feature in our day 281 spectrum of SN 2009dc is the broad, double-peaked line centred near 7200 Å, which was also the strongest feature detected in a spectrum of SN 2006gz from 338 d past maximum (Maeda et al. 2009). In late-time spectra of SNe Ia this is attributed to blends of various [Fe II] lines, whereas in core-collapse SNe it is associated with [Ca II] λλ7291, 7324, though in a late-time spectrum of SN 2006gz it has been suggested that the feature is due to a combination of both [Fe II] and [Ca II] lines (Maeda et al. 2009). The shape of the profile in SN 2009dc matches roughly that of SN 1998bu (though the central dip in SN 2009dc is deeper), but differs somewhat significantly from that of SN 1990N. Shapes similar to the one seen in SN 2009dc have, however, been seen by Maeda et al. (2009), who present synthetic late-time spectra of SNe Ia. Their models with more massive progenitors seem to lead to the feature near 7200 Å becoming strong relative to the complex of lines in the range 3800–5500 Å, as seen in SN 2009dc.

3.4.5 SN 2009dc and SN 2002cx-like objects

As already mentioned numerous times, SN 2009dc shares some interesting properties with both SN 2002cx and SN 2005hk, which are members of a class of peculiar SNe Ia (Filippenko 2003; Li et al. 2003b; Jha et al. 2006). These so-called 'SN 2002cx-like' SNe are characterized by low expansion velocities and low peak luminosities, slow late-time declines in *R* and Fe III features dominating early-time spectra (Jha et al. 2006). Many of these criteria hold for SN 2009dc as well, but the very obvious difference is that the peak luminosity of SN 2009dc is much larger than average (see Section 4.1) while those of SN 2002cx-like objects are well below average.

In Section 3.1, we noted the absence of a prominent second maximum in the *R*- and *I*-band light curves of SN 2009dc. This lack of a secondary maximum has been observed in SN 2002cx-like objects (Li et al. 2003b; Phillips et al. 2007). However, as seen in Fig. 2, SN 2005hk (an SN 2002cx-like object) evolves much faster than SN 2009dc in all bands and proves to be a poor match photometrically. The colour indices of SN 2009dc and SN 2005hk are again a poor match as shown in Fig. 5.

Spectroscopically, SN 2009dc does not really resemble SN 2002cx-like objects before maximum (see Fig. 6), nor about 9 months after maximum (see Fig. 12). At these latest times, the

spectrum of SN 2009dc consists of broad emission from forbidden iron lines while the spectrum of SN 2002cx is made up of many *narrow permitted* lines of Fe II, Na II, Ca II and (tentatively) O I (Jha et al. 2006). This is supported by the fact that the narrow spectral features of SN 2002cx do not simply appear to correspond to resolved versions of the blends seen in SN 2009dc.

Despite all of these differences, we have shown that at 1–2 months past maximum brightness the spectra of SN 2009dc and SN 2002cx are surprisingly similar. In Fig. 9 we have combined the day 20 and 25 spectra of SN 2002cx from Li et al. (2003b) in order to improve the S/N and the wavelength coverage. Not only are the overall shapes of these two spectra nearly identical, but the width, strength and existence of almost all of the individual spectral features match extremely well (with one significant exception, the Si II λ6355 absorption as mentioned in Section 3.4.1). Both objects, after being dereddened and deredshifted, appear to have an underlying blackbody continuum of about 5500 K (Branch et al. 2004).

About a month past maximum, Li et al. (2003b) and Branch et al. (2004) calculate expansion velocities of $\sim$5000–6000 km s^{-1} for SN 2002cx, and Phillips et al. (2007) determine expansion velocities in nearly the same range for SN 2005hk. For SN 2009dc we also derive velocities in this range for a few ions (O I, Ca II, Fe II and Si II) with significant uncertainty since not only are many of these features blended, but the line identifications themselves are not definitive. These values also match well with the expansion velocity of $\sim$6000 km s^{-1} derived by Yamanaka et al. (2009) from their spectrum of SN 2009dc from 25 d past maximum.

Both Li et al. (2003b) and Branch et al. (2004) determine an expansion velocity for SN 2002cx at 56 d past maximum of $\sim$4700 km s^{-1} based on the Fe II λ4555 feature and a SYNOW fit. Phillips et al. (2007) calculate a slightly higher value of about 6000 km s^{-1} for SN 2005hk at 55 d past maximum (also using the Fe II λ4555 line). Based on this Fe II feature, we determine an expansion velocity of $\sim$5500 km s^{-1} for our spectra of SN 2009dc from 52 and 64 d past maximum. If we use the Si II λ6355 line, which is still present in SN 2009dc but not seen in the SN 2002cx-like objects, we derive similar expansion velocities for both our day 52 and day 64 spectra. In general, it appears that the post-maximum expansion velocities of the spectral features of SN 2009dc are slightly greater than those seen in SN 2002cx by a few hundred km s^{-1} depending on the feature (Li et al. 2003b; Branch et al. 2004), whereas they are about equal to those of SN 2005hk (Phillips et al. 2007).

In conclusion, SN 2009dc and SN 2002cx-like objects have quite different photometric properties but are nearly identical spectroscopically *only* at 1–2 months past maximum brightness. The expansion velocity, the blackbody temperature and the chemical composition match extremely well at these epochs, but the evolution of these observables from pre-maximum to nearly a year after maximum is quite different between SN 2009dc and SN 2002cx-like objects.

3.4.6 SN 2007if

In Fig. 13, we present our late-time spectra of another possible SC SN Ia, SN 2007if. As noted earlier, the spectra of SN 2007if generally look similar to those of SN 2009dc, SN 2002cx and even SN 2005cf at comparable epochs. The most significant spectral differences between SN 2007if and SN 2009dc are, as stated previously, that the expansion velocities seen in SN 2007if are $\sim$1000 km s^{-1} larger than those in SN 2009dc and SN 2002cx at

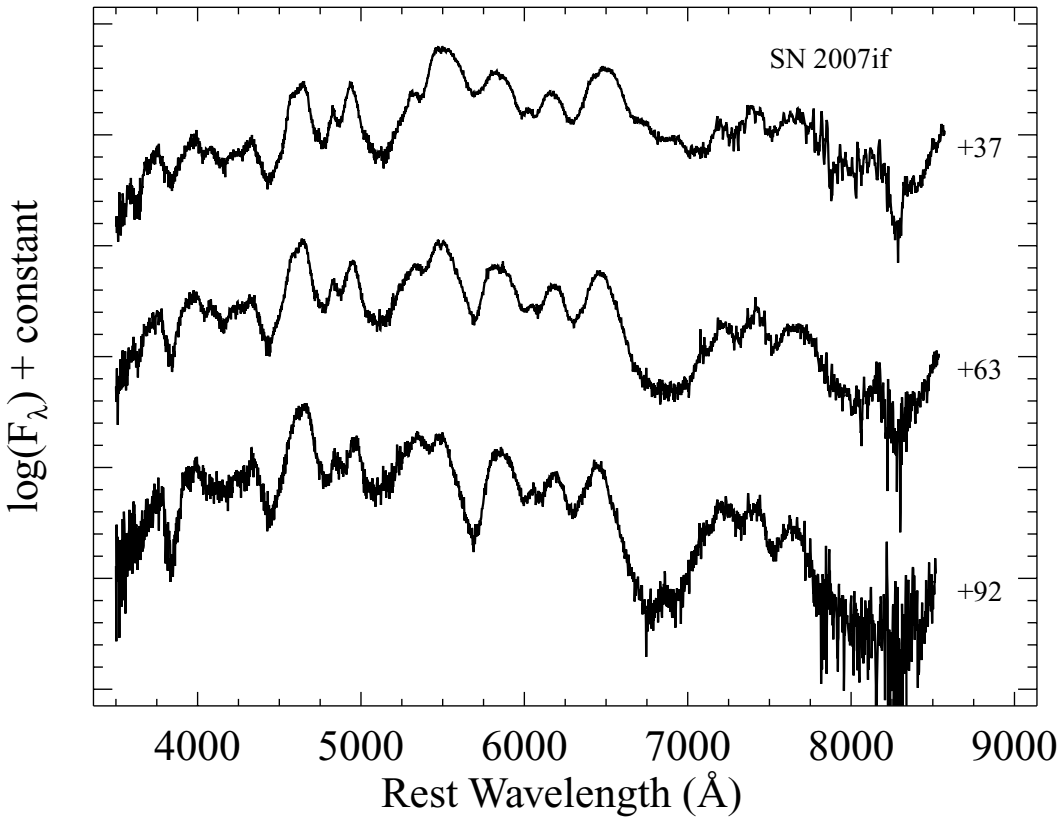

Figure 13. Our spectra of SN 2007if with days relative to maximum light indicated in each case. We have removed the host-galaxy recession velocity (cz = 22 200 $\pm$ 250 km s^{-1}, Scalzo et al. 2010).

comparable phases. This larger velocity is likely causing some of the medium-width features seen in SN 2009dc and SN 2002cx to be 'smoothed out', and hence we do not detect many of these features in SN 2007if. It also has velocities which are smaller than those seen in SN 2005cf, but otherwise the spectra match well.

We have also stated previously that SN 2007if does not show the strong Si II λ6355 absorption after maximum that is visible in spectra of SN 2009dc (as well as in SN 2005cf). Unfortunately, our observations of SN 2007if do not extend to sufficiently long wavelengths for us to inspect whether the Ca II near-IR triplet of SN 2007if shows the complex structure seen in SN 2009dc.

The main aspects of the spectral evolution of SN 2007if over our three epochs is the disappearance of broad emission near 5500 Å and in the ranges 6700–7100 Å and possibly 7800–8100 Å (though our data are noisy in this second range of wavelengths). These match nearly exactly with the spectral features of SN 2009dc that were seen to decrease in strength over similar epochs.[6]

3.5 Reddening and extinction

As mentioned above, we detect weak (but noticeable), narrow absorption from Na I D in all of our spectra of SN 2009dc, both at zero redshift and at the recession velocity of the SN itself ($cz = 6300 \pm 300$ km s^{-1}). Even though there are clear notches in all of our spectra at the correct wavelengths for Na I D in the MW and in the host of SN 2009dc (UGC 10064), they are not broader than our spectral resolution.

We attempt to measure an EW of both absorption features in each of our observations, and we calculate average values of $\sim$0.7 ± 0.1 Å for the MW and $\sim$1.0 ± 0.1 Å for UGC 10064. These are close to the values of 0.7 and 1.2 Å reported by Marion et al. (2009) and 0.5 and 1.0 Å found by Tanaka et al. (2010).

There is some uncertainty in how exactly to convert the EW of Na I D absorption into extinction, but a few (mainly empirical) relations do exist (e.g. Barbon et al. 1990; Munari & Zwitter 1997; Turatto, Benetti & Cappellaro 2003). Using these conversions, we determine a range of values for $E(B-V)$ both in the MW ($0.1 \lesssim E(B-V)_{\rm MW} \lesssim 0.18$ mag) and in UGC 10064 [$0.15 \lesssim E(B-V)_{\rm host} \lesssim 0.3$ mag].

For the extinction from the MW, we compare our calculated values of $E(B-V)$ to the value from the Galactic dust maps of Schlegel et al. (1998). Their maps give $E(B-V)_{\rm MW} = 0.070$ mag for the position of SN 2009dc, slightly lower than our range of values. However, since the accuracy of the Schlegel et al. (1998) dust maps is almost certainly higher than that of our EW measurements, we adopt $E(B-V)_{\rm MW} = 0.070$ mag for our analysis.

The extinction from UGC 10064 is a bit more complicated to determine accurately. If the Lira–Phillips relation holds for SN 2009dc, then we expect an extinction of $E(B-V)_{\rm host} \approx 0.26$ mag (see Section 3.2 for details on our application of the Lira–Phillips relation), which is within our range of values calculated from the spectra. Furthermore, if we assume that the EW of Na I D is directly proportional to $E(B-V)$, as Tanaka et al. (2010) do, then we derive $E(B-V)_{\rm host} \approx (1.0/0.7\ \text{Å}) \times 0.070 \approx 0.1$ mag. Taking into account all of these values, their uncertainties, and the method by which they were derived, we adopt $E(B-V)_{\rm host} = 0.1$ mag for our analysis, which is our lowest plausible, non-zero reddening. However, we note that the reddening could be as large as 0.3 mag.

[6] The third wavelength range which possibly decreased in strength in SN 2009dc, 7800–8100 Å, is outside of our spectral coverage of SN 2007if.

3.6 Host-galaxy properties

SN 2009dc occurred $\sim$27 arcsec away from the centre of the S0 galaxy UGC 10064. We adopt the luminosity distance ($d_{\rm L}$) as the distance to the SN, again assuming a ΛCDM Universe with $H_0 = 70$ km s^{-1} Mpc^{-1}, $\Omega_{\rm m} = 0.27$ and $\Omega_\Lambda = 0.73$ (Spergel et al. 2007) and $z = 0.022 \pm 0.001$, where the redshift has been corrected for infall into the Virgo cluster, and we have adopted an uncertainty of $cz = 300$ km s^{-1} to allow for a peculiar velocity induced by the gravitational interaction of neighbouring galaxies. At $d_{\rm L} = 97 \pm 7$ Mpc, SN 2009dc is a projected distance of $\sim$13 kpc from the centre of UGC 10064. A useful galactic scale is the radius containing 50 per cent of the flux (Petrosian 1976), which for UGC 10064 is about 4.71 ± 0.21 arcsec in the R band (Abazajian et al. 2009). This puts SN 2009dc about 5.7 Petrosian radii (in projection) from the centre of its host. For comparison, SN 2003fg was found to be projected 0.9 kpc from the core of its low-mass star-forming host (Howell et al. 2006) and SN 2007if was discovered effectively directly on top of its low-mass and low-metallicity host (Scalzo et al. 2010). The host of SN 2006gz is an Scd galaxy, and the SN was projected 14.4 kpc from the nucleus (Hicken et al. 2007), while SN 2004gu was projected 2.21 kpc from its host's nucleus (Monard et al. 2004). It seems that host-galaxy type and distance from the nucleus vary widely among candidate SC SN Ia (though the distance comparison is difficult given projection effects). However, SN 2003fg, SN 2007if and possibly SN 2009dc (see below) were all associated with regions of recent star formation.

Wegner & Grogin (2008) inspected an optical spectrum of the core of UGC 10064 and derived an age of 4.0 ± 3.0 Gyr, a metallicity [Z/H] = 0.45 ± 0.07 and a chemical abundance [α/Fe] = 0.13 ± 0.09. This value for metallicity is about 1σ above the average found for 26 S0/E void galaxies by Wegner & Grogin (2008), whereas the chemical abundance is just about the same as their average value. Optical spectra of the nucleus of UGC 10064 show no strong emission lines (Wegner & Grogin 2008; Abazajian et al. 2009), implying very little ongoing star formation ($\lesssim$0.2 M$_\odot$ yr^{-1}) in the core of the galaxy.

However, recent deep H I surveys of S0 galaxies have shown that the majority of non-cluster early-type galaxies contain substantial reservoirs (10^6–10^9 M$_\odot$) of neutral gas that extend to large galactocentric radii (Morganti et al. 2006), whose morphology and kinematics suggest external origins. On the other hand, in the majority of these galaxies the column density of this gas is too low to support star formation at large radii, and thus the stellar populations throughout the galaxy are old.

Interestingly, in a fraction of the early-type galaxies rich in H I, a dynamical feature such as a prominent bar can create relatively dense ring-like accumulations of neutral gas at large radii (e.g. Schinnerer & Scoville 2002; Weijmans et al. 2008). In these regions of enhanced H I, low-level star formation ($\sim$0.1 M$_\odot$ yr^{-1}) is observed (Jeong et al. 2007; Shapiro et al. 2010). Since SN 2009dc exploded in the outskirts of an S0 galaxy, it seems difficult to say with certainty whether SN 2009dc came from an old or young stellar population.

In the Supplementary Information of Howell et al. (2006), the age of the host galaxy of SN 2003fg is estimated to be $\sim$700 Myr (with significant uncertainty) and the star formation rate to be $1.26^{+0.02}_{-1}$ M$_\odot$ yr^{-1}, averaged over 0.5 Gyr. This star formation rate is nearly an order of magnitude greater than the value derived by Wegner & Grogin (2008) for the core of UGC 10064 as well as the residual star formation rate seen in rings of enhanced neutral gas at large galactocentric radii (Jeong et al. 2007; Shapiro et al. 2010). SC

SNe Ia are expected to be found preferentially in young stellar populations (e.g. Howell et al. 2006; Chen & Li 2009, and references therein), but they are not necessarily restricted to them. If SC SNe Ia are the result of the merger of two degenerate objects, then the merger time-scale can be set by the emission of gravitational waves (e.g. Iben & Tutukov 1984). Depending on the particular orbital parameters of the binary, there may be a significant delay between the formation of the constituent degenerate objects and their eventual merger. Thus, SC SNe Ia *could* occur in older stellar populations.

Even though there is a significant difference between the average star formation rates near the sites of SN 2009dc and SN 2003fg, there is still a possibility that they both come from relatively young stellar populations. As mentioned above, an age of ∼700 Myr was calculated for the environment of SN 2003fg (Howell et al. 2006, Supplementary Information), while an age of ∼4.0 Gyr was calculated for the *core* of the host of SN 2009dc (Wegner & Grogin 2008). The fact that SN 2009dc is a few effective radii away from the nucleus of its host, coupled with the observations of low levels of residual star formation in other early-type galaxies at such galactocentric radii, implies that it is possible that SN 2009dc also came from a relatively small, but young, stellar population on the edge of UGC 10064, and that the age calculated for the core of the galaxy is not actually representative of the local environment of SN 2009dc.

Furthermore, in the SDSS Data Release 7, an extended, blue source appears 99.3 arcsec (which is a projected distance of 43.6 kpc) to the north-west of UGC 10064 (Abazajian et al. 2009). This SBdm galaxy is known as SDSS J155108.42+254321.3 or UGC 10063 (de Vaucouleurs et al. 1991). *Swift*/UVOT images of the SN 2009dc field (shown in Fig. 14) indicate that UGC 10063 is significantly bluer than UGC 10064. The irregularly shaped UGC 10063 is barely visible in the KAIT *R*-band image to the north-west of SN 2009dc in Fig. 1. Stacked UVOT images show that UGC 10063 increases in prominence in progressively bluer bands. As seen in Fig. 14, UGC 10063 seems to have a tidal tail extending towards UGC 10064, pointed roughly at the site of SN 2009dc.

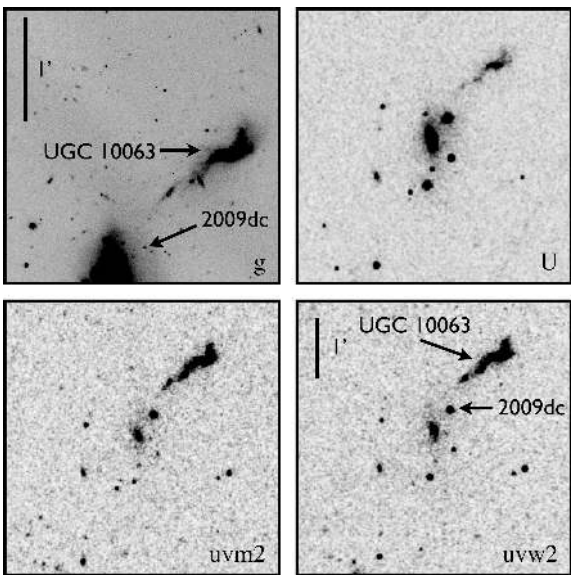

Figure 14. Keck *g*-band image and stacked UVOT *U*, *uvm*2 and *uvw*2 images of UGC 10063 (SDSS J155108.42+254321.3). UGC 10063 and SN 2009dc are labelled in the upper-left and lower-right panels. The upper-left panel is 2.69 × 2.69 arcmin^2, and the remaining panels are 4.67 × 4.67 arcmin^2; north is up and east is to the left in all four images. UGC 10063 increases in prominence in progressively bluer bands, and is much bluer than UGC 10064 (compare its appearance here with that in Fig. 1). It also seems to have a tidal tail extending towards UGC 10064, pointed roughly in the direction of the site of SN 2009dc.

On 2010 Feb. 7 we obtained a spectrum of UGC 10063 using LRIS on the Keck I telescope (with a 1-arcsec-wide slit, a 600/4000 grism on the blue side and a 400/8500 grating on the red side, resulting in FWHM resolutions of ∼4 and ∼6 Å, respectively). It has a blue continuum with few spectral features, but there is strong and narrow absorption from the Balmer series (though Hα is undetected). Strong Balmer lines and the lack of obvious emission lines are the hallmarks of so-called 'post-starburst' galaxies in which vigorous star formation activity ended between ∼50 Myr and 1.5 Gyr ago (Poggianti et al. 2009, and references therein). This is consistent with UGC 10063 being a SBdm galaxy (de Vaucouleurs et al. 1991). From the seven Balmer absorption lines marked in Fig. 15, we calculate the redshift of UGC 10063 to be 0.021 ± 0.001, consistent with the redshift derived from the 21-cm H I line ($z = 0.02158 \pm 0.00003$; Schneider et al. 1990). This also exactly matches the redshift of UGC 10064 and SN 2009dc (as determined from narrow Ca II H&K absorption).

Based on the spectrum of UGC 10063 and its position relative to UGC 10064, we propose that these two galaxies had a close encounter in the relatively recent past. If UGC 10063 passed near the nucleus of UGC 10064, gas from UGC 10063 could have been stripped off and become gravitationally bound to UGC 10064 (which has been seen in both simulations and observations; e.g. Barnes & Hernquist 1991; Falcón-Barroso et al. 2004). This newly acquired gas (some of which could be at large galactocentric radii) would have likely undergone a burst of star formation soon after the two galaxies had their closest encounter (Mihos & Hernquist 1994; Barnes & Hernquist 1996), and this might be how and when the progenitor of SN 2009dc formed. Both SN 2007if and SN 2003fg were also found in hosts with recent star formation (Scalzo et al. 2010); in fact, SN 2003fg was discovered in a tidal feature (Howell et al. 2006) reminiscent of SN 2009dc and UGC 10063.

4 DISCUSSION

4.1 Bolometric luminosity

To estimate the bolometric luminosity of SN 2009dc, we follow the method outlined by Howell et al. (2009). Using spectra of SN 2009dc presented here and spectra of the similar SC SN Ia candidate SN 2007if from Scalzo et al. (2010), we take each simultaneous epoch of *BVRI* photometry and warp the spectrum closest in phase to match the photometry using a smooth third-order spline. We then integrate the warped spectrum over wavelengths of 4000–8800 Å (i.e. from the blue edge of the *B*-band filter to the red edge of *I*-band filter.) We convert the flux into a luminosity using the luminosity distance ($d_L = 97 \pm 7$ Mpc) adopted in Section 3.6.

The above method will only give us the optical bolometric luminosity. To derive the total bolometric luminosity from UV to IR, we use bolometric corrections from Wang et al. (2009b), who found that *BVRI* only accounts for ∼60 per cent of the total luminosity in the case of SN 2005cf, a normal SN Ia. They also found that an additional 20 per cent is emitted in the UV and *U* band, and the final 20 per cent in the near-IR. We test to see if the tabulated corrections

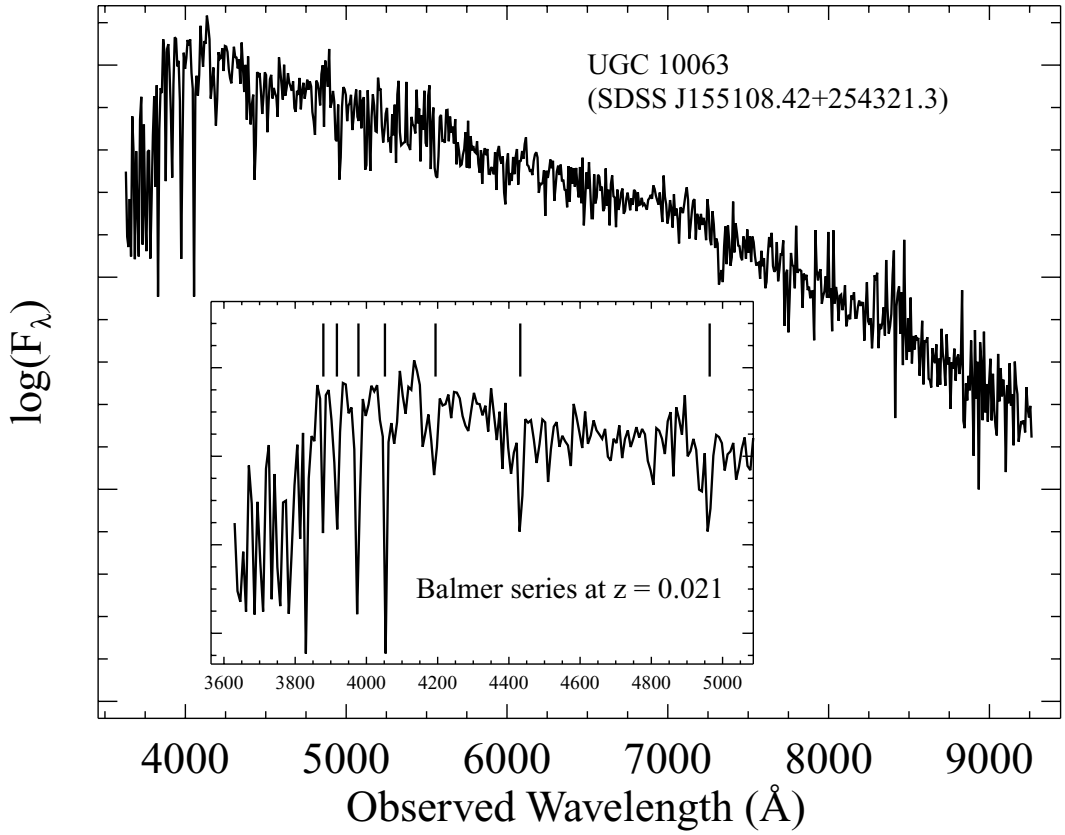

Figure 15. An optical spectrum of UGC 10063 (SDSS J155108.42+254321.3). The inset is a zoom-in of the full spectrum. Narrow Balmer-series absorption (Hβ through Hθ) is marked, and these features yield $z = 0.021 \pm 0.001$, equal to the redshift of UGC 10064 and SN 2009dc. Note that Hα is undetected at an expected wavelength of ∼6700 Å; perhaps Hα emission from residual H II regions fills in the absorption line.

for the UV and *U* band are reasonable for SN 2009dc by first calculating the bolometric luminosity using optical and UV photometry at $t = 0$ d (using our optical ground-based photometry combined with UVOT photometry of SN 2009dc). We find that our results are consistent with a correction of 20 per cent. Yamanaka et al. (2009) found that their near-IR data for SN 2009dc represented ∼20 per cent of the bolometric luminosity. With this, we cautiously adopt a 40 per cent correction for our bolometric luminosity using our well-sampled *BVRI* photometry. Overall, SN 2005cf is a much different SN than SN 2009dc, so we include a systematic uncertainty of 20 per cent for our bolometric luminosity.

Fig. 16 shows our final bolometric light curves for the various levels of host-galaxy extinction we have adopted throughout this paper. We also plot the bolometric light curve of SN 2005cf for comparison.

If we use our fiducial non-zero value for the host-galaxy reddening, $E(B-V)_{\rm host} = 0.1$ mag, and our largest reasonable value for the host reddening, $E(B-V)_{\rm host} = 0.3$ mag, then we get $M_V = -20.16 \pm 0.1$ mag [$L_{\rm bol} = (3.3 \pm 0.6) \times 10^{43}$ erg s^{-1}] and $M_V = -20.82 \pm 0.10$ mag [$L_{\rm bol} = (7.3 \pm 1.0) \times 10^{43}$ erg s^{-1}], respectively. We note that assuming no host-galaxy extinction we find $M_V = -19.83 \pm 0.10$ mag [$L_{\rm bol} = (2.4 \pm 0.5) \times 10^{43}$ erg s^{-1}]. A summary of these results can be found in Table 7. Our range of values of $L_{\rm bol}$ for SN 2009dc matches quite well with that of Yamanaka et al. (2009): (2.1–3.3) $\times 10^{43}$ erg s^{-1}. The most significant difference between the two analyses comes from using a different range of values for $E(B-V)_{\rm host}$ and R_V.

4.2 ^{56}Ni masses and energetics

4.2.1 ^{56}Ni masses from Arnett's law

The vast majority of the bolometric luminosity of SNe Ia comes from the decay of ^{56}Ni to ^{56}Co (and subsequently the decay of ^{56}Co to ^{56}Fe), so we can calculate how much ^{56}Ni was created in SN 2009dc by using 'Arnett's law', which asserts that the luminosity of an SN Ia at maximum light is proportional to the instantaneous rate of radioactive decay of ^{56}Ni (e.g. Arnett 1982; Stritzinger & Leibundgut 2005). Arnett's law is often written as

$$M_{\rm Ni} = \frac{L_{\rm bol}}{\alpha \dot{S}(t_{\rm R})}, \quad (1)$$

where $M_{\rm Ni}$ is the mass of ^{56}Ni present in the ejecta, $L_{\rm bol}$ is the bolometric luminosity at maximum light, α is the ratio of bolometric to radioactive luminosities (which is of the order of unity) and $\dot{S}(t_{\rm R})$ is the radioactive luminosity per mass of ^{56}Ni as a function of the rise time, $t_{\rm R}$.

For SN 2009dc, we have tight constraints on the rise time from our photometric data and, as described in Section 3.1, we find a value of 23 ± 2 d. Substituting this into the equation for $\dot{S}(t_{\rm R})$ from Stritzinger & Leibundgut (2005), we get $\dot{S}(t_{\rm R}) \approx (1.65 \pm 0.13) \times 10^{43}$ erg s^{-1} M$_\odot^{-1}$. Stritzinger & Leibundgut (2005) find $\alpha = 1.2 \pm 0.2$, which we use for our analysis, though we note that this is an upper limit (which leads to a lower limit on the ^{56}Ni mass) since any ^{56}Ni that is *above* the photosphere will not contribute to the SN luminosity.

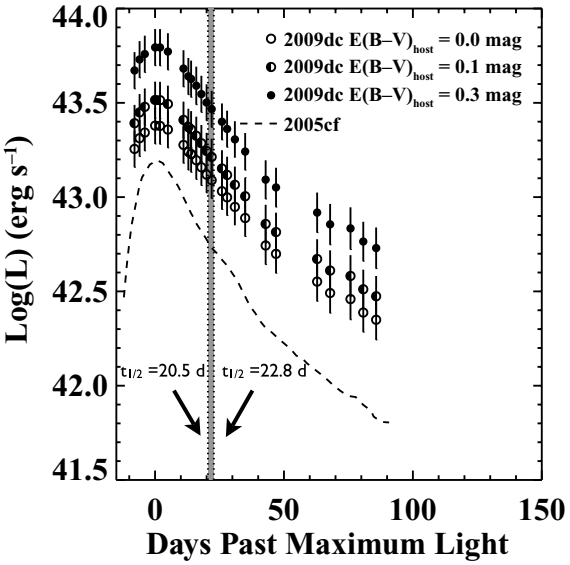

Figure 16. Bolometric light curve of SN 2009dc assuming various levels of extinction, in comparison with that of SN 2005cf. The curve plotted with empty circles assumes no host-galaxy extinction, the half-filled circles assume $E(B-V)_{\rm host} = 0.1$ mag with $R_V = 3.1$, and the filled circles assume $E(B-V)_{\rm host} = 0.3$ mag with $R_V = 3.1$. For comparison, we include the bolometric light curve of SN 2005cf as a dashed line (Wang et al. 2009b). We indicate our calculated range of values of $t_{+1/2}$ (i.e. the number of days after maximum bolometric luminosity when the bolometric luminosity has decreased to half its maximum value) for SN 2009dc within the shaded grey region bounded by dotted lines. The lower bound of $t_{+1/2} = 20.5$ d is calculated using a host reddening of $E(B-V)_{\rm host} = 0.3$ mag and the upper limit of $t_{+1/2} = 22.8$ d assumes no host-galaxy extinction.

Table 7. Bolometric luminosity for various reddenings.

$E(B-V)_{\rm host}$ (mag)	$L_{\rm bol,max}$ (10^{43} erg s^{-1})	$M_{V,\rm max}$ (mag)
0.0	2.4 ± 0.5	-19.83 ± 0.10
0.1	3.3 ± 0.6	-20.16 ± 0.10
0.3	7.3 ± 1.0	-20.82 ± 0.10

Using these values, along with our most likely estimate of the bolometric luminosity mentioned above, we calculate that SN 2009dc synthesised about 1.7 ± 0.4 M$_\odot$ of ^{56}Ni. If we adopt the bolometric luminosity assuming no host-galaxy reddening and our largest reasonable host-galaxy reddening, along with our calculated rise time and $\alpha = 1.2$, we get $\sim$1.2 M$_\odot$ and $\sim$3.7 M$_\odot$ of ^{56}Ni, respectively.

4.2.2 ^{56}Ni masses from late-time photometry

The detection of SN 2009dc in late-time images at levels similar to those of normal SNe Ia offers a stark contrast to SN 2006gz, another SC SN Ia candidate. Late-time photometry obtained by Maeda et al. (2009) $\sim$360 d after maximum found that SN 2006gz had faded significantly faster than normal SNe Ia, casting doubt on the amount of ^{56}Ni synthesized in the explosion. The authors constrain $M_{\rm Ni} \lesssim 0.3$ M$_\odot$ assuming that the positrons are nearly completely trapped in the ejecta. This is at odds with the $\sim$1 M$_\odot$ of ^{56}Ni calculated to power the light curve at early times (Hicken et al. 2007).[7] To reconcile this difference in nickel mass, it was suggested that perhaps SN 2006gz was a highly asymmetric explosion, and due to the exact viewing angle more ^{56}Ni was inferred at early times than was actually present (Maeda et al. 2009). However, SN 2009dc appears to be spherically symmetric at early times (Tanaka et al. 2010). Furthermore, Maeda et al. (2009) posit that dust might have formed in the ejecta of SN 2006gz by this time, which would reprocess much of the optical light to longer wavelengths. However, we do not see strong evidence for dust formation in SN 2009dc since the spectral features all appear to evolve symmetrically.

Table 8. Ni mass estimates from late-time photometry.

Days past explosion	$f_{\rm e^+}$	$E(B-V)_{\rm host}$ (mag)	$L_{\rm bol}$ [a] (10^{40} erg s^{-1})	^{56}Ni (M$_\odot$)
304	0.75	0	3.1 ± 0.7	1.4 ± 0.3
304	1	0	3.1 ± 0.7	1.0 ± 0.2
304	0.75	0.1	4.2 ± 0.8	1.8 ± 0.3
304	1	0.1	4.2 ± 0.8	1.4 ± 0.3
304	0.75	0.3	7.9 ± 1.5	3.4 ± 0.6
304	1	0.3	7.9 ± 1.5	2.5 ± 0.6
426	0.75	0	0.26 ± 0.05	0.33 ± 0.06
426	1	0	0.26 ± 0.05	0.25 ± 0.05
426	0.75	0.1	0.35 ± 0.07	0.45 ± 0.08
426	1	0.1	0.35 ± 0.07	0.34 ± 0.06
426	0.75	0.3	0.64 ± 0.12	0.82 ± 0.15
426	1	0.3	0.64 ± 0.12	0.62 ± 0.12

[a]Bolometric luminosity only contains contribution over the range 4000–8800 Å.

To constrain the nickel mass produced by SN 2009dc from late-time photometry, we write out the SN luminosity as a function of time (e.g. Clocchiatti & Wheeler 1997; Maeda et al. 2003, 2009),

$$L(t) = M_{\rm Ni}\left(\varepsilon_\gamma(1-{\rm e}^{-\tau(t)}) + f_{\rm e^+}\varepsilon_{\rm e^+}\right){\rm e}^{-t/111.3} \quad (2)$$

where t is the number of days from the explosion date, $M_{\rm Ni}$ is the initial amount of ^{56}Ni synthesized, $\varepsilon_\gamma = 6.8 \times 10^9$ erg s^{-1} g^{-1}, $\tau(t)$ is the time-dependent optical depth to γ-rays, $f_{\rm e^+}$ is the fraction of positrons trapped in the ejecta, $\varepsilon_{\rm e^+} = 2.4 \times 10^8$ erg s^{-1} g^{-1}, and 111.3 d is the e-folding time of ^{56}Co decay. Evaluating $\tau(t)$ requires defining a model with estimates for the kinetic energy of the explosion and the total mass of the WD.

We can place constraints on the ^{56}Ni mass by only considering the luminosity powered by the trapped positrons; to do this we set $\tau(t) = 0$ in equation (2). Using only the optical contribution to the bolometric luminosity over the range 4000–8000 Å from our Keck data taken 281 d past maximum (which is 304 d after explosion), we calculate the ^{56}Ni mass for a number of reddening and $f_{\rm e^+}$ values which can be found in Table 8. Our calculation of the bolometric luminosity does not include a bolometric correction for any possible contribution to the bolometric luminosity in the NIR. For our nominal values of $E(B-V)_{\rm host} = 0.1$ mag, $R_V = 3.1$ and $f_{\rm e^+} = 1$, we calculate a ^{56}Ni mass of 1.4 ± 0.3 M$_\odot$, consistent with the ^{56}Ni mass derived from Arnett's law and our data at $B_{\rm max}$ (Section 4.2.1).

We also determine the ^{56}Ni mass using our epoch of photometry from 403 d past maximum (which is 426 d after explosion). However, without a spectrum to model the spectral energy distribution at this phase, we had to use our last spectrum taken 281 d past

[7] Note that this value was derived by assuming a high value for the host-galaxy reddening of SN 2006gz, which might have been an overestimate.

B_{max}, which could lead to an inaccurate measure of the bolometric luminosity. Furthermore, the detection of the SN was marginal in all bands. Using our nominal values of $E(B-V)_{host} = 0.1$ mag, $R_V = 3.1$ and $f_{e^+} = 1$, we calculate a ^{56}Ni mass of 0.34 ± 0.06 $M_\odot$, clearly much lower than previous estimates of the ^{56}Ni mass. We summarize ^{56}Ni masses for a range of parameters in Table 8.

The drop in derived ^{56}Ni mass and expected luminosity could indicate the formation of dust between $t = 281$ and 426 d past maximum light, although this cannot be substantiated without IR data or a relatively high S/N spectrum. The unexpected drop could also be an indication that the positron trapping fraction at this phase is significantly lower than the nominal value of $f_{e^+} = 1$. To produce the $\sim$1.4 $M_\odot$ of ^{56}Ni found using our photometry from 281 d past maximum, we would need $f_{e^+} \approx 0.25$. SN 2009dc could have undergone an 'IR catastrophe' which would cause most of the emission to escape at IR wavelengths (as opposed to the optical; Axelrod 1988) as the temperature of the SN cools to $\sim$1000 K. This would require using a bolometric correction to our derived optical bolometric luminosity. Alternatively, the low derived ^{56}Ni mass could suggest that the late-time light curve of SN 2009dc is not powered by the decay of ^{56}Co. This conclusion, however, is at odds with the ^{56}Ni mass derived from our epoch of photometry from $t = 281$ d past maximum light. Without near-IR data or a spectrum at this epoch, it is difficult to reconcile these differences. We again caution that the spectral energy distribution is ill constrained at this phase.

4.2.3 WD masses and kinetic energies

Using the technique developed by Howell et al. (2006), we attempt to combine our observations of SN 2009dc with properties of WDs and SNe Ia in order to calculate the mass of the progenitor WD as well as the amount of ^{56}Ni produced in the explosion. We note that this method is independent of the one used in the previous section which utilized the late-time photometry of SN 2009dc. As will be mentioned below, there are a few assumptions and simplifications that go into this analysis, and thus the final values should probably not be taken literally. However, the sense of the relationships and trends these calculations indicate should be reliable and will show that SN 2009dc likely had an SC WD progenitor.

The ejecta of SNe Ia derive their kinetic energy (E_K) from the energy released during explosive nucleosynthesis (E_n), but the ejecta must first overcome the binding energy (E_b) of the WD progenitor (Branch 1992). Therefore, we can write

$$E_K = \frac{M_{WD} v^2}{2} = E_n - E_b, \quad (3)$$

where M_{WD} is the mass of the WD just before explosion and v is a representative velocity of the ejecta. A single value for velocity only relates to the kinetic energy of the SN averaged over the entire ejecta, and thus there has been disagreement as to which actual value should be used for a given SN. Previous studies have used the velocity of the Si II λ6355 feature at 10 and 40 d past maximum (Benetti et al. 2005; Howell et al. 2006).

Since about 70 per cent of IGEs produced in SNe Ia are in the form of ^{56}Ni (Nomoto, Thielemann & Yokoi 1984; Khokhlov, Mueller & Höflich 1993), the total mass of the WD can be related to the nickel mass by

$$M_{Ni} = 0.7 M_{WD} f_{IGE}, \quad (4)$$

where f_{IGE} is the fractional composition of IGEs in the SN ejecta. However, the exact amount of IGEs that are made up of ^{56}Ni may not be the same for all SNe Ia and likely dependent on other, external factors such as metallicity (e.g. Howell et al. 2009, and references therein).

Furthermore, Branch (1992) found that fusing equal parts carbon and oxygen all the way to iron yields $\varepsilon_{Fe} = 1.55 \times 10^{51}$ erg $M_\odot^{-1}$, and burning the same material only up to silicon liberates about 76 per cent of that energy. Thus we can write

$$E_n = \varepsilon_{Fe} M_{WD} (f_{IGE} + 0.76 f_{IME}), \quad (5)$$

where f_{IME} is the fractional composition of IMEs in the ejecta.

Finally, we define the fractional composition of unburned carbon in the SN ejecta as f_C.[8] Based on our definitions we can write

$$1 = f_C + f_{IME} + f_{IGE}. \quad (6)$$

Putting all of this together, we relate various properties of the progenitor WD to properties of the SN ejecta it created using

$$v^2 \approx 2\varepsilon_{Fe} \left(\frac{0.34 M_{Ni}}{M_{WD}} - 0.76 f_C + 0.76 \right) - \frac{2E_b}{M_{WD}}. \quad (7)$$

However, given the assumptions and simplifications that went into this 'equation', we stress that it should be used more as an illustration of how the different parameters relate to each other and less as a tool to actually calculate WD and ^{56}Ni masses.

Values of E_b range from about 0.5×10^{51} erg for a WD with a mass of 1.4 $M_\odot$ to about 1.3×10^{51} erg for a WD with a mass of 2 $M_\odot$ and a central density of 4×10^9 g cm^{-3} (Yoon & Langer 2005). We perform separate calculations for each pair of these values of E_b and M_{WD}. Tanaka et al. (2010) measure the Si II λ6355 feature to be blueshifted by 7200 km s^{-1} in their spectrum of SN 2009dc obtained 6 d past maximum, while we find the same feature to be blueshifted by 5000–6000 km s^{-1} in our spectra taken 35, 52 and 64 d past maximum. Since v has been evaluated at 10 and 40 d past maximum for similar analyses previously (Benetti et al. 2005; Howell et al. 2006), we will use a range of velocities from 7000 km s^{-1} to 5500 km s^{-1} for our analysis. Finally, since there is clear indication of unburned material in the ejecta of SN 2009dc (see Section 3.3.2), we know that f_C must be non-zero. However, based on models of SN Ia ejecta (e.g. Nomoto et al. 1984) and the relative scarcity of carbon detections in SNe Ia (Marion et al. 2006; Thomas et al. 2007), we will only use values in the range 0.05–0.3 for f_C.

With such large uncertainties and so many parameters, we will clearly calculate a huge range of ^{56}Ni masses, and we realize that a few assumptions and model-dependent values have come into the derivation. However, this is still a useful line of reasoning in our attempt to determine both the mass of the WD progenitor and the amount of ^{56}Ni synthesized by SN 2009dc. We therefore forge ahead and attempt to eliminate at least some of the most extreme situations.

Almost all of parameter space is ruled out when we use a 1.4 $M_\odot$ WD (and its associated binding energy), since we calculate negative nickel masses for these cases. The largest ^{56}Ni mass we can reasonably derive for a 1.4 $M_\odot$ WD (using $f_C = 0.3$ and $v = 7000$ km s^{-1}) is 0.06 $M_\odot$, nearly an order of magnitude smaller than the amount of nickel produced by a normal SN Ia (e.g. Nomoto et al. 1984; Kasen et al. 2008). We have also shown that SN 2009dc is much more luminous than the average SN Ia. Therefore, if it did have a 1.4 $M_\odot$ progenitor, then we would need to invoke a large,

[8] This parameter does not appear in the equation for E_n; it represents the amount of *unburned* material, and thus does not contribute to the energy released by nucleosynthesis.

hitherto unknown energy source to power its light curve, which seems highly unlikely.

The situation changes when we use a 2 $M_\odot$ WD (with a central density of 4×10^9 g cm^{-3}), put forth as a possible SC SN Ia progenitor by Yoon & Langer (2005). Again, a significant part of parameter space is eliminated, since at low values of f_C we calculate negative (or extremely small) nickel masses. Assuming that f_{IME} must be $\gtrsim$0.1 (given that we detect IMEs in the spectra for months after maximum; see e.g. Nomoto et al. 1984), we calculate nickel masses as high as $\sim$1 $M_\odot$. In order to match our nominal ^{56}Ni mass range of 1.4–1.7 $M_\odot$ *and* satisfy our constraints on the fractional composition of elements mentioned previously, we must resort to using a WD progenitor more massive than 2 $M_\odot$.

Again, the final values calculated above are almost certainly not the true answer. However, the range of plausible values presented, as well as the relationships between the parameters of the SN and its WD progenitor, yet again indicates that the progenitor of SN 2009dc was likely an SC WD.

The various analyses presented above seem to strongly favour the conclusion that the progenitor of SN 2009dc was an SC WD with a mass of probably greater than $\sim$2 $M_\odot$. These analyses also indicate that SN 2009dc most likely produced 1.4–1.7 $M_\odot$ of ^{56}Ni (assuming our nominal value for the host-galaxy reddening and our peak bolometric luminosity). More than 1 $M_\odot$ of ^{56}Ni was almost certainly created by SN 2009dc, and the actual value *could* be as high as $\sim$3.3 $M_\odot$. This matches well with the conclusions of Yamanaka et al. (2009), who calculate a similar range of nickel masses for SN 2009dc (1.2–1.8 $M_\odot$). Part of the difference can be accounted for by the fact that the two studies use different values of host-galaxy reddening (causing the derived bolometric luminosities to differ somewhat; see Section 4.1). However, the majority of the difference in derived ^{56}Ni masses comes from the assumed rise time of SN 2009dc. Yamanaka et al. (2009) adopt a rise time of 20 d based on comparisons to typical SNe Ia and SN 2006gz, while we use a rise time of 23 d based on our pre-maximum photometry. The longer rise time used in our study leads to a larger derived nickel mass for SN 2009dc.

SN 2003fg had a derived progenitor mass of $\sim$2.1 $M_\odot$ and produced $\sim$1.3 $M_\odot$ of ^{56}Ni (Howell et al. 2006), and these values are quite similar to those we calculate for SN 2009dc. SN 2006gz was estimated to have produced 1–1.2 $M_\odot$ of ^{56}Ni, which is on the low end of our range for SN 2009dc, and it was also claimed to have an SC WD progenitor (though no attempt was made to further constrain the progenitor mass; Hicken et al. 2007).

4.3 Comparison to theoretical models

Any theoretical model which is postulated to explain SN 2009dc, with or without a SC WD, *must* be able to reproduce the observed peculiarities for which we have very tight constraints: (i) high luminosity even when assuming no host-galaxy reddening, (ii) relatively long light-curve rise time, (iii) relatively slow photometric decline and late-time spectroscopic evolution, (iv) the presence of carbon in spectra near maximum brightness, (v) the presence of silicon in spectra as late as a few months past maximum brightness, (vi) IGEs dominating the spectra at late times and (vii) mostly spherically symmetric ejecta near maximum with possible clumpy layers of IMEs (Tanaka et al. 2010).

Below, we consider both SC and non-SC models, all of which involve the thermonuclear explosion of a WD. However, the similarities between SN 2009dc and SN 2002cx and its brethren (see Section 3.4.5) may argue that the progenitor and explosion scenario for these objects are all linked. Could SN 2009dc be an SN 2002cx-like object but with a much higher luminosity? Perhaps, although attempts to explain the origins of even the best-observed SN 2002cx-like objects are still ongoing (e.g. Jha et al. 2006; Phillips et al. 2007; Valenti et al. 2009; Li et al., in preparation).

4.3.1 SC models

Two- and three-dimensional models of differentially rotating massive WDs have been presented in the literature, and calculations show that SC WDs with masses as large as 2 $M_\odot$ are possible by accretion from a non-degenerate companion, while masses up to $\sim$1.5 $M_\odot$ are possible from a double-degenerate merger (Yoon & Langer 2005; Yoon, Podsiadlowski & Rosswog 2007, respectively). More recent studies of double-degenerate mergers have even shown possible SN Ia progenitors with total masses approaching 2.4 $M_\odot$ (Greggio 2010). This is encouraging for the case of SN 2009dc, since our energetics arguments imply that its progenitor is likely greater than $\sim$2 $M_\odot$. However, calculations by Piro (2008) suggest that differential rotation is unlikely for WDs accreting from a non-degenerate companion, and thus their masses cannot exceed the Chandrasekhar mass by more than a few per cent.

Yoon & Langer (2005) also consider how much ^{56}Ni would be produced by an SN Ia whose progenitor is $\sim$2 $M_\odot$, calculating values of 0.4–1.3 $M_\odot$. This large range does encompass the lower end of our range of ^{56}Ni for SN 2009dc. However, only specific kinetic energies (i.e. kinetic energies per unit mass) which are lower than what we find for SN 2009dc by a factor of $\sim$2 were used (Yoon & Langer 2005). Adopting lower specific kinetic energies will tend to decrease the nickel yield for a given WD mass, according to their models. It is possible that increasing the specific kinetic energies used in the models of Yoon & Langer (2005) to values that better match SN 2009dc will in fact reproduce our derived nickel mass, but this may require pushing the models into regimes where they are no longer valid.

Pfannes, Niemeyer & Schmidt (2010) use aspects of the WD models of Yoon & Langer (2005) and simulate prompt detonations of massive, rapidly rotating WDs. None of their models appears to reproduce the fact that we detect unburned fuel (i.e., carbon) and IMEs near maximum brightness at low velocities, and subsequently IMEs and IGEs at later times (also at low velocities). Even more at odds with SN 2009dc, Pfannes et al. (2010) predict that the IMEs and unburned material should have similar spatial distributions in the ejecta (specifically, in a torus in the equatorial plane), but this seems unlikely given the strong line polarizations seen by Tanaka et al. (2010) in Si II and Ca II features and the lack thereof in two different C II features. Thus, we conclude that the models of Pfannes et al. (2010) do not seem to reproduce the observations of SN 2009dc.

Models of SC WDs and their evolution in close binary systems with non-degenerate companions can also be found in the literature (Chen & Li 2009). These evolutionary calculations include the effects of varying the orbital period of the binary systems, the metallicity and mass-transfer rate of the binary companion, and (most importantly) the mass of the WD. Chen & Li (2009) find that WDs with initial masses of $\sim$1.2 $M_\odot$, under the right mass-transfer conditions, can accrete up to masses of about 1.4–1.8 $M_\odot$ before exploding as an SN Ia (though they find that most of these WDs explode with masses not much above 1.4 $M_\odot$). Thus it seems somewhat unlikely that these models can explain the progenitor we suggest for SN 2009dc; even if the occasional WD *can* accrete up to 1.8 $M_\odot$, this is at the lowest end of our range of WD progenitor masses.

Spherically symmetric, one-dimensional radiation transport calculations for normal and SC WDs have been carried out by Maeda & Iwamoto (2009). They find that based on the light-curve shapes, photospheric velocities, peak bolometric luminosities and peak effective temperatures, SN 2006gz likely came from an SC WD[9] while SN 2003fg did not. Since the observables of SN 2003fg used for their analysis have very similar values to those of SN 2009dc, it would seem that their models imply that SN 2009dc is also not an SC SN Ia. Maeda & Iwamoto (2009) point out that SN 2003fg (and thus probably SN 2009dc as well) could be an SC SN Ia if the progenitor star were highly aspherical, but again this seems unlikely for SN 2009dc from the spectropolarimetric data (Tanaka et al. 2010).

The primary independent variable used in the calculations of Maeda & Iwamoto (2009) is $t_{+1/2}$, the number of days after maximum bolometric luminosity when the bolometric luminosity has decreased to half its maximum value (Contardo, Leibundgut & Vacca 2000). For SN 2006gz they measure $t_{+1/2} = 18$ d from the publicly available photometry, but for SN 2003fg they convert the stretch value published by Howell et al. (2006) to Δm_{15} and then to a $t_{+1/2}$ value of 13.5 d (adopting an empirical linear fit to Δm_{15} and $t_{+1/2}$ values from Contardo et al. 2000). Using their conversions between Δm_{15} and $t_{+1/2}$, we calculate $t_{+1/2} \approx 14$ d (which, unsurprisingly, is nearly the same as the value calculated for SN 2003fg by Maeda & Iwamoto 2009). However, when we measure $t_{+1/2}$ directly from our light curve, we get a minimum value of about 20.5 d (when we use our maximum plausible host-galaxy reddening), which is nearly 50 per cent larger! Furthermore, if one converts the Δm_{15} value of SN 2006gz to $t_{+1/2}$ using the linear fit, one again finds $t_{+1/2} \approx 14$ d, suggesting that the linear conversion derived by Maeda & Iwamoto (2009) is not accurate for such low values of Δm_{15}. This is not wholly unexpected since the Δm_{15} values of SNe 2006gz, 2003fg and 2009dc (or $t_{+1/2}$ as measured from light curves) are all below (or above) the values used to derive the linear fit (Contardo et al. 2000). In addition, the conversion from stretch to Δm_{15} used by Maeda & Iwamoto (2009) for SN 2003fg did not take into account the fact that the definition of stretch has evolved as new SN Ia light-curve templates have been constructed (e.g. Conley et al. 2008).

We can now compare SN 2009dc to the analysis of Maeda & Iwamoto (2009) using the actual values of $t_{+1/2} \approx 20.5$–22.8 d. Given the large bolometric luminosity and $t_{+1/2}$ value, as well as the extremely low photospheric velocity of SN 2009dc, none of their models (using normal or SC WDs) appears to be viable. Their 'normal WD' model with $M_{\rm WD} = 1.39$ M$_\odot$ and $M_{\rm Ni} = 0.6$ M$_\odot$ accounts for the low velocity with large $t_{+1/2}$, but it underpredicts $L_{\rm bol}$ by a factor of a few. Some of the SC WD models ($M_{\rm WD} \geqslant 2.0$ M$_\odot$ and $M_{\rm Ni} = 1.0$ M$_\odot$) of Maeda & Iwamoto (2009) can almost account for the large values of $L_{\rm bol}$ and $t_{+1/2}$ seen in SN 2009dc, but they then overpredict the photospheric velocity of SN 2009dc by a factor of 2 or so (with the models having the highest mass WDs coming the closest to matching the observed velocities).

While no single model of Maeda & Iwamoto (2009) clearly reproduces our observations of SN 2009dc, its properties seem to be on the outskirts of the parameter space explored by their analysis. This hints at the possibility that more extreme WD and ^{56}Ni masses may be required to match the observational data of SN 2009dc. In addition, it is possible that *multi-dimensional* analyses are required to truly capture the underlying physics of an SC WD explosion.

[9] Maeda & Iwamoto (2009) claim that most of the emission likely shifted to the near-IR and mid-IR at late times in order to explain the relatively faint late-time observations of Maeda et al. (2009).

Furthermore, a few synthetic late-time spectra of SC SNe Ia have been presented in the literature (e.g. Maeda et al. 2009). Their models take as inputs a WD progenitor mass, a WD central density and mass fractions of burning products, and then use a one-dimensional Monte Carlo radiation transport code, along with ionization/recombination equilibrium and rate equations, to calculate synthetic light curves and spectra. Both of their SC SN Ia models roughly match our SN 2009dc photometry. In addition, their late-time spectra are similar to our day 281 spectrum of SN 2009dc. Maeda et al. (2009) note that as they increase their models' progenitor mass, the [Fe II]/[Ca II] feature near 7200 Å becomes stronger relative to the blends of [Fe II] and [Fe III] near 3800–5500 Å. This is seen in SN 2009dc (as compared to SNe Ia with more normal peak luminosity), and it further supports our finding that the progenitor of SN 2009dc was an SC WD. However, it should be noted that the SC SN Ia models of Maeda et al. (2009) only use WDs with masses of 2 and 3 M$_\odot$, and ^{56}Ni masses of only 1 M$_\odot$, which is on the low end of our range of calculated values for the ^{56}Ni yield of SN 2009dc.

4.3.2 Non-SC models

A number of models which employ Chandrasekhar-mass WDs as the progenitors of super-luminous SNe Ia (ones that we would consider possibly SC SNe Ia) have been proposed (Hillebrandt, Sim & Röpke 2007; Sim et al. 2007; Kasen et al. 2008; Kasen, Röpke & Woosley 2009). These models usually invoke the off-centre ignition of a normal WD progenitor which leads to nuclear burning (and thus ^{56}Ni production) that is peaked away from the centre of the WD. This off-centre nickel blob would increase the observed luminosity if the blob were offset from the centre of the WD towards the observer, with the maximum effect occurring when it is offset directly along the line of sight. These viewing angles also lead to the fastest light-curve rise times in such simulations (Sim et al. 2007; Kasen et al. 2008).

Once again, we can compare our observed values for SN 2009dc to the models. Since the nickel blob is offset from the centre, asphericity is introduced into the explosion by construction (Kasen et al. 2008). If there is in fact a blob of ^{56}Ni in SN 2009dc and it is offset from the progenitor's centre directly along our line of sight (thus maximizing the measured luminosity), then perhaps there is still azimuthal symmetry in the explosion. This may account for the low levels of continuum polarization measured by Tanaka et al. (2010), as well as the higher levels of IME line polarization, but it seems tenuous at best.

Observing along the axis of the offset blob of ^{56}Ni, Hillebrandt et al. (2007) produce light curves that peak at a bolometric magnitude of $M_{\rm bol} \approx -19.9$ mag, Kasen et al. (2008) show light curves that get as bright as $M_B \approx -20$ mag and Kasen et al. (2009) claim models with luminosities as high as 2.1×10^{43} erg s^{-1}. These brightest magnitudes and luminosities that can be obtained by off-centre explosions are nearly equal to our *lower limits* for SN 2009dc (assuming no host-galaxy reddening), and are likely below the true values. Furthermore, we note that the maximum amount of ^{56}Ni obtained from these explosions is 0.9–1.1 M$_\odot$ (Hillebrandt et al. 2007; Kasen et al. 2009), which is once again at the lowest end of our range of calculated values for SN 2009dc.

Finally, as mentioned above, the viewing angles that maximize the observed peak magnitudes also *minimize* the rise time. We find a relatively long rise time of 23 ± 2 d for SN 2009dc, and our first detection of the SN implies that its rise time *must be* >21 d. This is

significantly longer than the rise times for these viewing angles as derived from the models (∼12 and ∼18 d; Hillebrandt et al. 2007; Kasen et al. 2008, respectively). Thus, it seems that none of these models which include a Chandrasekhar-mass WD is viable for SN 2009dc.

It should be mentioned, however, that these models mostly assume expansion velocities of 'normal' SNe Ia (e.g. Sim et al. 2007) and we have shown that the expansion velocity of SN 2009dc is significantly lower. This is evident in the synthetic spectra derived from these models; from all viewing angles, they resemble early-time normal SN Ia spectra much more than the spectra of SN 2009dc near maximum brightness (Kasen et al. 2008). Thus, perhaps it is not too surprising that these specific examples of non-SC models do not match the observations of SN 2009dc.

5 CONCLUSIONS

In this paper, we have presented and analysed optical photometry and spectra of SN 2009dc and SN 2007if, both of which are possibly SC SNe Ia. Our photometric and spectral data on SN 2009dc constitute one of the richest data sets ever published on an SC SN Ia candidate. Our well-sampled light curve follows SN 2009dc from about 1 week before maximum brightness until about 5 months past maximum, and shows that SN 2009dc is one of the slowest photometrically evolving SNe Ia ever observed. We derive a rise time of 23 d and $\Delta m_{15}(B) = 0.72$ mag, which are two of the most extreme values for these parameters ever seen in an SN Ia. Assuming no host-galaxy reddening, we derive a peak bolometric luminosity of about 2.4×10^{43} erg s^{-1}, though this is almost certainly an underestimate since we observe strong evidence for at lease *some* host reddening. Using our non-zero values for $E(B-V)_{\rm host}$, the peak bolometric luminosity increases by about 40 to 200 per cent.

Spectroscopically, SN 2009dc also evolves relatively slowly. Strong C II absorption features (which are rarely observed in SNe Ia) are seen in the spectra near maximum brightness, implying a significant amount of unburned fuel from the progenitor WD in the outer layers of the SN ejecta. Si II absorption also appears in our spectra of SN 2009dc and remains visible even 2 months past maximum. Our post-maximum spectra are dominated by a forest of IGE features and, interestingly, resemble spectra of the peculiar SN Ia 2002cx. Finally, the spectra of SN 2009dc all show very low expansion velocities at all layers (i.e. unburned carbon, IMEs and IGEs) as compared to other SNe Ia. This may be explained by a massive WD progenitor which consequently has a large binding energy. Even though the expansion velocities are small, we see no strong evidence in SN 2009dc for a velocity 'plateau' near maximum light like the one seen in SN 2007if (Scalzo et al. 2010).

Using various luminosity and energy arguments, we calculate that the progenitor of SN 2009dc is possibly an SC WD with a mass greater than ∼2 $M_\odot$, and that at least ∼1 $M_\odot$ of ^{56}Ni was likely formed in the explosion (though the most probable value is in the range 1.4–1.7 $M_\odot$). These values are larger than (or about as large as) those calculated for any other SN Ia ever observed. We propose that the host galaxy of SN 2009dc underwent a gravitational interaction with a nearby galaxy (UGC 10063) in the relatively recent past, and that this could have induced a sudden burst of star formation which may have given rise to the progenitor of SN 2009dc and turned UGC 10063 into the 'post-starburst' galaxy that we observe today. We also compare our observed quantities for SN 2009dc to theoretical models, and while no model seems to match or explain every aspect of SN 2009dc, simulations show that SC WDs with masses near what we calculate for the progenitor of SN 2009dc can possibly form, likely from the merger of two WDs. Furthermore, models of extremely luminous SNe Ia which employ a Chandrasekhar-mass WD progenitor cannot explain our observations of SN 2009dc.

Thus, taking all of these extreme values into account, we conclude that SN 2009dc is very likely an SC SN Ia. As mentioned previously, many of the observed peculiarities of SN 2009dc are also seen in SN 2003fg and SN 2007if. Therefore, we concur with Howell et al. (2006) and Scalzo et al. (2010) that both SN 2003fg and SN 2007if (respectively) are also probably SC SNe Ia. However, given their fairly normal expansion velocities and relative weakness (or even absence) of C II features near maximum brightness, it seems that SN 2006gz and SN 2004gu are less likely to be SC SNe Ia.

New large transient searches such as Pan-STARRS (Kaiser et al. 2002) and the Palomar Transient Factory (Rau et al. 2009; Law et al. 2009) will probably find many SC or other super-luminous SNe Ia in the near future. Since it seems that they cannot be standardized in the same way as most SNe Ia, they will need to be handled separately or ignored in cosmological surveys which will use large numbers of SNe Ia. However, the simulations of Chen & Li (2009) show that donor stars with lower metallicities (e.g. Population II stars) are less likely to form WDs with masses greater than 1.7 $M_\odot$ than higher metallicity stars. Thus, it is possible that contamination levels from SC SNe Ia, which are already rare at low redshifts (i.e., average metallicity), may be relatively small in medium or high-redshift surveys.

ACKNOWLEDGMENTS

We thank P. F. Hopkins, K. M. Sandstrom and K. L. Shapiro for useful discussions regarding host galaxies. We are especially grateful to D. A. Howell for the near-maximum spectrum of SN 2003fg (and, as the referee, for many useful comments), K. Maeda for the late-time spectrum of SN 2006gz, R. A. Scalzo and P. E. Nugent for information regarding SN 2007if, and M. Yamanaka for early-time comparison photometry of SN 2009dc. We also thank I. Arcavi, S. B. Cenko, J. Choi, B. E. Cobb, R. J. Foley, C. V. Griffith, M. T. Kandrashoff, M. Kislak, I. K. W. Kleiser, J. Leja, M. Modjaz, A. J. L. Morton, J. Rex, T. N. Steele, P. Thrasher and X. Wang for their assistance with some of the observations and data reduction, as well as J. Kong, N. Lee and E. Miller for their help in improving and maintaining the SNDB. We are grateful to the staff at the Lick and Keck Observatories for their support. Some of the data presented herein were obtained at the W. M. Keck Observatory, which is operated as a scientific partnership among the California Institute of Technology, the University of California, and the National Aeronautics and Space Administration (NASA); the observatory was made possible by the generous financial support of the W. M. Keck Foundation. The authors wish to recognize and acknowledge the very significant cultural role and reverence that the summit of Mauna Kea has always had within the indigenous Hawaiian community; we are most fortunate to have the opportunity to conduct observations from this mountain. This research has made use of the NASA/IPAC Extragalactic Data base (NED) which is operated by the Jet Propulsion Laboratory, California Institute of Technology, under contract with NASA. AVF's group is supported by the NSF grant AST-0908886, DOE grants DE-FC02-06ER41453 (SciDAC) and DE-FG02-08ER41563, NASA/*Swift* grant NNX09AL08G, and the TABASGO Foundation. KAIT and its ongoing operation were made possible by donations from Sun Microsystems, Inc., the Hewlett-Packard Company, AutoScope Corporation, Lick Observatory, the NSF, the University of California, the Sylvia & Jim

Katzman Foundation and the TABASGO Foundation. JMS is grateful to Marc J. Staley for a Graduate Fellowship.

REFERENCES

Abazajian K. N. et al., 2009, ApJS, 182, 543
Amanullah R. et al., 2010, ApJ, 716, 712
Arnett W. D., 1982, ApJ, 253, 785
Axelrod T. S., 1988, in Nomoto K., ed., Atmospheric Diagnostics of Stellar Evolution. Lecture Notes in Physics. Springer, Berlin, p. 375
Barbon R., Benetti S., Rosino L., Cappellaro E., Turatto M., 1990, A&A, 237, 79
Barnes J. E., Hernquist L. E., 1991, ApJ, 370, L65
Barnes J. E., Hernquist L. E., 1996, ApJ, 471, 115
Benetti S. et al., 2005, ApJ, 623, 1011
Branch D., 1992, ApJ, 392, 35
Branch D. et al., 2003, AJ, 126, 1489
Branch D., Baron E., Thomas R. C., Kasen D., Li W., Filippenko A. V., 2004, PASP, 116, 903
Cardelli J. A., Clayton G. C., Mathis J. S., 1989, ApJ, 345, 245
Chen W., Li X., 2009, ApJ, 702, 686
Chornock R., Filippenko A. V., 2008, AJ, 136, 2227
Chornock R., Filippenko A. V., Branch D., Foley R. J., Jha S., Li W., 2006, PASP, 118, 722
Clocchiatti A., Wheeler J. C., 1997, ApJ, 491, 375
Conley A. et al., 2008, ApJ, 681, 482
Contardo G., Leibundgut B., Vacca W. D., 2000, A&A, 359, 876
Contreras C. et al., 2010, AJ, 139, 519
de Vaucouleurs G. et al., 1991, Third Reference Catalogue of Bright Galaxies. Springer, New York
Faber S. M. et al., 2003, in Iye M., Moorwood A. F. M., eds, Proc. SPIE Conf. p. 1657
Falcón-Barroso J. et al., 2004, MNRAS, 350, 35
Filippenko A. V., 1982, PASP, 94, 715
Filippenko A. V., 1997, ARA&A, 35, 309
Filippenko A. V., 2003, in Hillebrandt W., Leibundgut B., eds, From Twilight to Highlight: The Physics of Supernovae. Springer-Verlag, Berlin, p. 171
Filippenko A. V. et al., 1992, ApJ, 384, L15
Filippenko A. V., Li W. D., Treffers R. R., Modjaz M., 2001, in Paczyński B., Chen W. P., Lemme C., eds, Small-Telescope Astronomy on Global Scales. Astron. Soc. Pac., San Francisco, p. 121
Fisher A., Branch D., Nugent P., Baron E., 1997, ApJ, 481, L89
Foley R. J. et al., 2003, PASP, 115, 1220
Foley R. J. et al., 2010, ApJ, 708, L61
Ganeshalingam M. et al., 2010, submitted
Gómez G., López R., 1998, AJ, 115, 1096
Greggio L., 2010, MNRAS, 406, 22
Hachinger S., Mazzali P. A., Benetti S., 2006, MNRAS, 370, 299
Hamuy M., Phillips M. M., Suntzeff N. B., Schommer R. A., Maza J., Smith R. C., Lira P., Aviles R., 1996, AJ, 112, 2438
Harutyunyan A., Elias-Rosa N., Benetti S., 2009, Central Bureau Astron. Telegrams, 1768, 1
Hayden B. T. et al., 2010, ApJ, 712, 350
Hicken M., Garnavich P. M., Prieto J. L., Blondin S., DePoy D. L., Kirshner R. P., Parrent J., 2007, ApJ, 669, L17
Hicken M. et al., 2009, ApJ, 700, 1097
Hillebrandt W., Sim S. A., Röpke F. K., 2007, A&A, 465, L17
Horne K., 1986, PASP, 98, 609
Howell D. A. et al., 2006, Nat, 443, 308
Howell D. A. et al., 2009, ApJ, 691, 661
Iben I., Jr, Tutukov A. V., 1984, ApJS, 54, 335
Jeong H., Bureau M., Yi S. K., Krajnović D., Davies R. L., 2007, MNRAS, 376, 1021
Jester S. et al., 2005, AJ, 130, 873
Jha S., Branch D., Chornock R., Foley R. J., Li W., Swift B. J., Casebeer D., Filippenko A. V., 2006, AJ, 132, 189
Jha S., Riess A. G., Kirshner R. P., 2007, ApJ, 659, 122
Kaiser N. et al., 2002, Proc. SPIE, 4836, 154
Kasen D., 2006, ApJ, 649, 939
Kasen D., Thomas R. C., Röpke F., Woosley S. E., 2008, J. Phys. Conf. Series, 125, 012007
Kasen D., Röpke F. K., Woosley S. E., 2009, Nat, 460, 869
Kessler R. et al., 2009, ApJS, 185, 32
Khokhlov A., Mueller E., Höflich P., 1993, A&A, 270, 223
Kowalski M. et al., 2008, ApJ, 686, 749
Kuchner M. J., Kirshner R. P., Pinto P. A., Leibundgut B., 1994, ApJ, 426, L89
Landolt A. U., 1992, AJ, 104, 340
Law N. M. et al., 2009, PASP, 121, 1395
Leibundgut B., 2000, A&AR, 10, 179
Leonard D. C., Li W., Filippenko A. V., Foley R. J., Chornock R., 2005, ApJ, 632, 450
Li W. D. et al., 2000, in Holt S. S., Zhang W. W., eds, Cosmic Explosions. AIP, New York, p. 103
Li W., Filippenko A. V., Chornock R., Jha S., 2003a, PASP, 115, 844
Li W. et al., 2003b, PASP, 115, 453
Li W., Jha S., Filippenko A. V., Bloom J. S., Pooley D., Foley R. J., Perley D. A., 2006, PASP, 118, 37
Lira P., 1996, Master's thesis, Univ. Chile
Lira P. et al., 1998, AJ, 115, 234
Maeda K., Iwamoto K., 2009, MNRAS, 394, 239
Maeda K., Mazzali P. A., Deng J., Nomoto K., Yoshii Y., Tomita H., Kobayashi Y., 2003, ApJ, 593, 931
Maeda K., Kawabata K., Li W., Tanaka M., Mazzali P. A., Hattori T., Nomoto K., Filippenko A. V., 2009, ApJ, 690, 1745
Marion G. H., Höflich P., Wheeler J. C., Robinson E. L., Gerardy C. L., Vacca W. D., 2006, ApJ, 645, 1392
Marion H., Garnavich P., Challis P., Calkins M., Peters W., 2009, CBET, 1776, 1
Matheson T., Filippenko A. V., Ho L. C., Barth A. J., Leonard D. C., 2000, AJ, 120, 1499
Mazzali P. A., Danziger I. J., Turatto M., 1995, A&A, 297, 509
Mazzali P. A., Chugai N., Turatto M., Lucy L. B., Danziger I. J., Cappellaro E., Della Valle M., Benetti S., 1997, MNRAS, 284, 151
Mazzali P. A., Cappellaro E., Danziger I. J., Turatto M., Benetti S., 1998, ApJ, 499, L49
Mihos J. C., Hernquist L., 1994, ApJ, 431, L9
Miller J. S., Stone R. P. S., 1993, Lick Obs. Tech. Rep. 66. Lick Obs., Santa Cruz
Monard L. A. G., Quimby R., Gerardy C., Höflich P., Wheeler J. C., Chen Y., Smith H. J., Bauer A., 2004, IAU Circ., 8454, 1
Morganti R. et al., 2006, MNRAS, 371, 157
Munari U., Zwitter T., 1997, A&A, 318, 269
Nobili S. et al., 2005, A&A, 437, 789
Nomoto K., Thielemann F., Yokoi K., 1984, ApJ, 286, 644
Nugent P., Phillips M., Baron E., Branch D., Hauschildt P., 1995, ApJ, 455, L147
Oke J. B. et al., 1995, PASP, 107, 375
Patat F., Benetti S., Cappellaro E., Danziger I. J., Della Valle M., Mazzali P. A., Turatto M., 1996, MNRAS, 278, 111
Perlmutter S. et al., 1999, ApJ, 517, 565
Petrosian V., 1976, ApJ, 209, L1
Pfannes J. M. M., Niemeyer J. C., Schmidt W., 2010, A&A, 509, 75
Phillips M. M., 1993, ApJ, 413, L105
Phillips M. M., Lira P., Suntzeff N. B., Schommer R. A., Hamuy M., Maza J., 1999, AJ, 118, 1766
Phillips M. M. et al., 2007, PASP, 119, 360
Piro A. L., 2008, ApJ, 679, 616
Poggianti B. M. et al., 2009, ApJ, 693, 112
Poole T. S. et al., 2008, MNRAS, 383, 627
Puckett T., Moore R., Newton J., Orff T., 2009, CBET, 1762, 1
Rau A. et al., 2009, PASP, 121, 1334
Riess A. G. et al., 1998, AJ, 116, 1009
Riess A. G. et al., 1999, AJ, 118, 2675
Ruiz-Lapuente P., Kirshner R. P., Phillips M. M., Challis P. M., Schmidt B. P., Filippenko A. V., Wheeler J. C., 1995, ApJ, 439, 60

Scalzo R. A. et al., 2010, ApJ, 713, 1073
Schinnerer E., Scoville N., 2002, ApJ, 577, L103
Schlegel D. J., Finkbeiner D. P., Davis M., 1998, ApJ, 500, 525
Schneider S. E. et al., 1990, ApJS, 72, 245
Shapiro K. L. et al., 2010, MNRAS, 402, 2140
Sim S. A., Sauer D. N., Röpke F. K., Hillebrandt W., 2007, MNRAS, 378, 2
Simon J. D. et al., 2009, ApJ, 702, 1157
Spergel D. N. et al., 2007, ApJS, 170, 377
Stanishev V. et al., 2007, A&A, 469, 645
Stritzinger M., Leibundgut B., 2005, A&A, 431, 423
Tanaka M. et al., 2008, ApJ, 677, 448
Tanaka M. et al., 2010, ApJ, 714, 1209
Thomas R. C. et al., 2007, ApJ, 654, L53
Turatto M., Benetti S., Cappellaro E., 2003, in Hillebrandt W., Leibundgut B., eds, From Twilight to Highlight: The Physics of Supernovae. Springer, Berlin, p. 200
Valenti S. et al., 2009, Nat, 459, 674
Wade R. A., Horne K., 1988, ApJ, 324, 411
Wang X. et al., 2009a, ApJ, 699, L139
Wang X. et al., 2009b, ApJ, 697, 380
Webbink R. F., 1984, ApJ, 277, 355
Wegner G., Grogin N. A., 2008, AJ, 136, 1
Weijmans A., Krajnović D., van de Ven G., Oosterloo T. A., Morganti R., de Zeeuw P. T., 2008, MNRAS, 383, 1343
Whelan J., Iben I., Jr, 1973, ApJ, 186, 1007
Yamanaka M. et al., 2009, ApJ, 707, L118
Yoon S., Langer N., 2005, A&A, 435, 967
Yoon S., Podsiadlowski P., Rosswog S., 2007, MNRAS, 380, 933

This paper has been typeset from a TEX/LATEX file prepared by the author.